Mathematical Biosciences and Engineering

MBE, 18 (4): 3092–3143.
DOI: 10.3934/mbe.2021155
Received: 06 February 2021
Accepted: 25 March 2021
Published: 02 April 2021

http://www.aimspress.com/journal/MBE

Research article

Multilevel thresholding using a modified ant lion optimizer with opposition-based learning for color image segmentation

Shikai Wang[1,*], Kangjian Sun[2], Wanying Zhang[2] and Heming Jia[3]

[1] School of Mathematical Sciences, Harbin Normal University, Harbin 150025, China
[2] College of Mechanical and Electrical Engineering, Northeast Forestry University, Harbin 150040, China
[3] College of Information Engineering, Sanming University, Sanming 365004, China

* **Correspondence:** Email: wangshikai510@163.com.

Abstract: Multilevel thresholding has important research value in image segmentation and can effectively solve region analysis problems of complex images. In this paper, Otsu and Kapur's entropy are adopted among thresholding segmentation methods. They are used as the objective functions. When the number of threshold increases, the time complexity increases exponentially. In order to overcome this drawback, a modified ant lion optimizer algorithm based on opposition-based learning (MALO) is proposed to determine the optimum threshold values by the maximization of the objective functions. By introducing the opposition-based learning strategy, the search accuracy and convergence performance are increased. In addition to IEEE CEC 2017 benchmark functions validation, 11 state-of-the-art algorithms are selected for comparison. A series of experiments are conducted to evaluate the segmentation performance of the algorithm. The evaluation metrics include: fitness value, peak signal-to-noise ratio, structural similarity index, feature similarity index, and computational time. The experimental data are analyzed and discussed in details. The experimental results significantly demonstrate that the proposed method is superior over others, which can be considered as a powerful and efficient thresholding technique.

Keywords: image segmentation; multilevel thresholding; Otsu; Kapur's entropy; ant lion optimizer; opposition-based learning

1. Introduction

With the emergence of computer technology, image processing has been widely used in many fields. Image segmentation is one of the classical topics in image processing [1]. It divides the original image into multiple sub-regions according to intensity, color, texture, and other attributes of the image [2]. Image segmentation is often the preprocessing phase of higher-class processing such as: image analysis, object recognition, and computer vision. Consequently, the performance of higher-class processing system depends on the accuracy of the segmentation technique adopted [3]. Researchers have proposed a range of segmentations, including edge detection, histogram based thresholding, region, feature clustering, and neural networks [4–6]. Histogram based thresholding is a simple and the most commonly used image segmentation method [7,8]. Thresholding methods can be divided into two categories: bi-level thresholding and multi-level thresholding. Bi-level thresholding means that the target and background can be clearly distinguished by a single threshold value. Multi-level thresholding denotes that the given image can be segmented into various classes by multiple threshold values [9–11].

Among available image thresholding techniques, Otsu and Kapur's entropy are two state-of-the-art thresholding methods [12–14]. Otsu and Kapur's entropy find the optimal threshold values according to some preset criteria. Otsu maximizes the variance of the histogram classes, and Kapur's entropy maximizes the entropy of the histogram. These thresholding techniques mentioned above can be easily extended to multilevel thresholding segmentation. However, the exhaustive search makes it inefficient to find the optimal threshold values, and the time complexity increases exponentially when the number of threshold increases. In order to overcome the above drawback, swarm intelligence (SI) algorithms are extensively used in multilevel thresholding problems [15,16]. Ibrahim et al. proposed the fish images segmentation model based on salp swarm algorithm, in which Otsu method is used to determine the threshold and extract fish from the original image [17]. Ouadfel et al. studied two metaheuristic algorithms: flower pollination algorithm and social spiders optimization. Then the performance of multilevel thresholding methods was evaluated comprehensively [18]. Infrared image is of great value in medical research. Díaz-Cortés applied dragonfly algorithm in medical image segmentation technology [19]. Satapathy et al. used Otsu method and a novel chaotic bat algorithm (CBA) to address bi-level and multi-level image thresholding problem. The chaotic map was considered to update the position of bat during the optimization search. The proposed CBA offered superior image quality measure values [20]. Salvi et al. presented an adaptive method for nuclei segmentation in H&E stained images, named multiscale adaptive nuclei analysis (MANA). High segmentation performances were obtained for different organ images [21]. Feng et al. invented a thresholding technique of 3D Otsu based on dimension decomposition rule. The test results on medical images showed that the proposed technique reduced time complexity without the loss of segmentation quality [22]. Zhao et al. proposed an improved ant colony optimizer (RCACO) using a random spare strategy and chaotic intensification strategy. The convergence speed and the convergence accuracy were main gains. Furthermore, it was also an excellent multilevel image segmentation algorithm [23]. In [24], the horizontal crossover search (HCS) and the vertical crossover search (VCS) were introduced into the ant colony optimizer for the first time. The proposed algorithm was named CCACO. The newly proposed algorithm was evaluated in the field of function optimization and image segmentation [24]. He et al. introduced the efficient krill herd (EKH) algorithm into image segmentation. The experimental results showed that the presented EKH algorithm was superior to the other algorithms [25]. Hilali-

Jaghdam et al. proposed a method based on the classical and quantum genetic algorithms to solve the medical images segmentation. The Genetic Algorithm (GA) used a binary coding while the Quantum Genetic Algorithm (QGA) used the qubit encoding of individuals [26]. Wu et al. proposed an improved teaching-learning-based optimization algorithm (DI-TLBO) and successfully applied it in casting X-ray image segmentation for multi-level threshold [27].

Mirjalili proposed a novel nature-inspired algorithm called ant lion optimizer (ALO) in 2015 [28]. Obviously, ALO algorithm simulates the intelligent behavior of antlions in nature, including building traps, catching preys, and rebuilding traps. In 2018, Hadidian-Moghaddam et al. used ALO algorithm to solve the optimal sizing and siting of distributed generation. The results showed that ALO had better performance than particle swarm optimization (PSO) and genetic algorithm (GA) in this field [29]. Raju et al. applied ALO algorithm for optimization of the controller gains. The results showed that the controller performed better in stabilization time(s), peak overshoot, and oscillations [30]. In 2016, by using ALO algorithm, Saxena et al. solved the problem of antenna current and antenna position optimization [31]. In the paper of Umaheswari et al., ALO was first adopted to solve the integrated maintenance scheduling problem [32]. Dinakara et al. proposed to determine the optimal distributed generation size by ALO. This approach achieved the purpose of reducing system power loss and improving voltage profile [33]. In [34], ALO was performed multilevel thresholding based on the contextual information of the image. Contextual information enhanced the quality of the segmented image as it considered not only the pixel value but also its vicinity. Jin et al. proposed a method to image segmentation based on ALO and fuzzy c-means (FCM). The proposed method alleviated the problem that the segmentation results of the images were unsatisfactory due to the presence of noise [35]. Yue et al. proposed an improved ALO called BIALO to enhance industrial images. Three strategies improved exploration and exploitation capabilities of the native algorithm [36]. In fact, there are still several disadvantages of the native ALO, such as the slow convergence rate, falling easily into local optimum and so on. In view of this phenomenon, it is necessary to improve the performance of the native ALO. In the paper of Wu et al., chaos was introduced into the initialization stage of ALO algorithm [37]. The improvement of ALO algorithm by Subhashini was to change the elite weight [38]. Majhi et al. proposed a hybrid clustering method based on k-means and ALO algorithm for cluster analysis in 2018 [39]. Some authors also include opposition-based learning (OBL) in their methods. This scheme can look for the opposite direction of each candidate solution. If the opposite point is beneficial then it is used as the candidate solution before proceeding to the next iteration. OBL helps in further exploration and better probability to converge to the optimum. Sarkhel et al. embedded OBL into harmony search algorithm, which improved the convergence rate of the algorithm [40]. Ewees et al. proposed a grasshopper optimization algorithm based on OBL strategy. Experimental results proved that the modified algorithm was competitive on engineering optimization problems [41]. In 2016, Ahandani et al. combined OBL with shuffled bidirectional differential evolution algorithm, which sped up the search process the algorithm [42].

Inspired by these successful applications of OBL strategy, OBL strategy is introduced into ALO algorithm to avoid falling into the local optimum. The search accuracy and convergence performance are improved. Then Otsu and Kapur's entropy as objective functions are maximized by MALO to find the optimum threshold values. Finally, the provided images are segmented into some classes. In this paper, IEEE CEC2017 benchmark functions [43] are used to evaluate the effectiveness of MALO. 7 traditional algorithms and 4 improved algorithms are selected for comparisons. The quality of the segmented images is evaluated in terms of fitness value, peak signal-to-noise ratio (PSNR) [44,45],

structural similarity index (SSIM) [46–48], feature similarity (FSIM) [49,50], and computational time. The experimental results confirm that the proposed method can be used effectively for multilevel thresholding.

The remainder of this paper is organized as follows: Section 2 outlines Otsu and Kapur's entropy methods for multilevel thresholding. Section 3 gives an overview of ALO followed by its mathematical model. ALO algorithm based on opposition-based learning for multilevel thresholding color image segmentation is presented in Section 4. Simulation experiments and results analysis are described in Section 5. Finally, Section 6 concludes the work and suggests some directions for future studies.

2. Materials and methods

Thresholding segmentation processes the histogram of digital images. An algorithm is used as the segmentation criterion. The threshold that satisfies the criterion function is called the optimal threshold. Based on the optimal threshold, the image is divided into target region and background region. The image thresholding method can be summarized into two categories: bi-level thresholding segmentation and multilevel thresholding segmentation. Bi-level thresholding segmentation cannot completely extract the target for a particular image. Multilevel thresholding divides the whole image into multiple regions. Multilevel thresholding segmentation can highlight the features among image regions.

The color image is represented by three different 8-bit gray values of R, G, and B channels. n_i denotes the number of pixels whose gray level is i. N denotes the total number of pixels. p_i denotes the distribution probability of the ith gray value. They are defined as follows:

$$N = \sum_{i=0}^{L-1} n_i \tag{1}$$

$$p_i = \frac{n_i}{N} \tag{2}$$

$$\sum_{i=0}^{L-1} p_i = 1 \tag{3}$$

Suppose there are K thresholds of $t_1, t_2, \cdots, t_K$. They divide the gray level of a given image into K+1 classes: $C_0 = [0, 1, \cdots, t_1\text{-}1], C_1 = [t_1, t_1 + 1, \cdots, t_2\text{-}1], C_K = [t_K, t_K + 1, \cdots, L\text{-}1]$.

The selection of threshold is related to the quality of the segmentation results. In this paper, Otsu and Kapur's entropy methods are adopted.

2.1. Otsu method

Otsu is an automatic threshold selection method for image segmentation, which was proposed in 1979. According to the grayscale characteristics of images, Otsu calculates the variance of class and determines the threshold. When the maximum variance of class is obtained, the threshold returned by the objective function is called the optimal threshold.

Equations (4)–(6) represent the probabilities of the class occurrence, the class mean levels, and the total mean level of the original image, respectively.

$$\omega_j = \sum_{i \in C_j} p_i \qquad j = 0, 1, \cdots, K. \tag{4}$$

$$\mu_j = \sum_{i \in C_j} \frac{ip_i}{\omega_j} \tag{5}$$

$$\mu_T = \sum_{i=0}^{L\text{-}1} ip_i \tag{6}$$

Then the total variance among the classes is：

$$\sigma^2(t_1, t_2, \cdots, t_K) = \sum_{j=0}^{k} \omega_j(\mu_j - \mu_T) \tag{7}$$

When $\sigma^2(t_1, t_2, \cdots, t_K)$ takes the maximum value, $(t_1^*, t_2^*, \cdots, t_k^*)$ is the optimal thresholding group of Otsu method.

2.2. Kapur's entropy method

In thresholding segmentation methods, Kapur's entropy method introduces the "entropy" of information theory into the segmentation. According to the additivity of entropy, the total entropy of the segmented image is:

$$\psi(t_1, t_2, \cdots t_K) = -\sum_{i=0}^{t_1\text{-}1} \frac{p_i}{P_0} \ln \frac{p_i}{P_0} - \sum_{i=t_1}^{t_2\text{-}1} \frac{p_i}{P_1} \ln \frac{p_i}{P_1} \cdots - \sum_{i=t_K}^{L\text{-}1} \frac{p_i}{P_K} \ln \frac{p_i}{P_K} \tag{8}$$

$$P_j = \sum_{i \in C_j} p_i \qquad j = 0, 1, \cdots, K. \tag{9}$$

where p_i is the distribution probability of the *i*th gray value, P_k is the probability of each class.

Kapur's entropy method finds the optimal threshold values based on maximizing the total entropy. The optimal threshold is determined by the following equation:

$$\left\{t_1^*, t_2^*, \cdots, t_K^*\right\} = \underset{0 < t_1 < t_2 \cdots < t_K < L\text{-}1}{argmax} \left(\psi(t_1, t_2, \cdots, t_K)\right) \tag{10}$$

3. Ant lion optimizer

3.1. Basic concepts

Ant lion optimizer is a novel swarm intelligent optimization algorithm. By simulating the process of antlion preying on ants in nature, the practical optimization problem is solved. The antlion uses its jaw to dig a cone-shaped pit in sand. After digging the trap, the antlion hides underneath the bottom of the cone. Random walks of ants may fall into it. Once an ant falls into trap, the antlion throws sand to

the edge of the pit and preys on it. After the antlion eats prey, it rebuilds its trap for the next hunt. Figure 1 shows several antlions and cone-shaped pits with different sizes. The details of the ALO algorithm are discussed as follows.

Figure 1. Antlions and cone-shaped pits with different sizes [28].

3.2. Mathematical model

Since ants move randomly in nature, the following equation is established to simulate the random movement of ants.

$$X(t) = [0, cumsum(2r(t_1) - 1), \cdots, cumsum(2r(t_n) - 1)] \tag{11}$$

where the $cumsum$ function evaluates the cumulative value of an array, $r(t)$ function is defined as follows:

$$r(t) = \begin{cases} 1 & if\ rand > 0.5 \\ 0 & if\ rand < 0.5 \end{cases} \tag{12}$$

where t shows the number of iterations in this study, $rand$ is a random number that belongs to [0,1].

In order to make random walks of ants in the search space, the following equation is needed to normalize Eq (11).

$$X_i^t = \frac{(X_i^t - a_i) \times (d_i^t - c_i^t)}{(b_i - a_i)} + c_i^t \tag{13}$$

where a_i denotes the minimum of random walk array $X(t)$, b_i denotes the maximum of random walk array $X(t)$, c_i^t denotes the lower boundary of ith space at tth iteration, and d_i^t denotes the upper boundary of ith space at tth iteration.

The ants move randomly around the antlion, and the boundary of the area is affected by the position of the antlion. The calculation equations of c_i^t and d_i^t are as follows:

$$c_i^t = Antlion_j^t + c^t \tag{14}$$

$$d_i^t = Antlion_j^t + d^t \tag{15}$$

where c_i^t denotes the lower boundary at *t*th iteration, and d_i^t is the upper boundary at *t*th iteration. $Antlion_j^t$ shows the position of the *j*th antlion at *t*th iteration by the roulette wheel selection.

Once the ant enters the trap, in order to prevent it from escaping, the antlion immediately digs out the sand outside the hole to make the ant slide into the bottom of the hole. This process can be seen as the decreasing radius of the ant random walk. The equations are as follows:

$$c^t = \frac{c^t}{I} \tag{16}$$

$$d^t = \frac{d^t}{I} \tag{17}$$

where *I* is the ratio of boundary contraction, and its equation is defined as follows:

$$I = 10^{\omega} \frac{t}{T} \tag{18}$$

where *t* is the current iteration, *T* is the maximum of iterations. ω is a fixed value, which can adjust the speed of ant moving to antlion.

According to the elite strategy, the antlion with the highest fitness value is considered as an elite, and the elite can affect the random walks of all ants. The antlion and the elite affect ant walking path. The ant's position update equation is as follows:

$$Ant_i^t = \frac{R_A^t + R_E^t}{2} \tag{19}$$

where R_A^t is an ant random walks around an antlion selected by roulette wheel, R_E^t is this ant random walks around the elite.

If the fitness of the updated ant is better than that selected antlion, which means that the ant is caught and eaten by the antlion. Then the position of the antlion is updated to this position of ant. The two equations are used as follows:

$$Antlion_j^t = Ant_i^t \quad if \quad f(Ant_i^t) > f(Antlion_j^t) \tag{20}$$

where Ant_i^t shows the *i*th ant with the best fitness value at *t*th iteration, and *f* is the fitness function value.

4. Proposed methods

ALO algorithm has drawbacks of falling easily into local optimum and lower search accuracy. In this section, a modified ALO algorithm is proposed. MALO uses opposition-based learning strategy to generate opposite solutions, which is helpful to search more effective regions. And then, MALO maximizes Otsu and Kapur's entropy methods to determine the optimal threshold.

4.1. Opposition based learning

Tizhoosh et al. proposed the concept of opposition-based learning in 2005. The main idea of this strategy is to generate opposite solutions. By comparing opposite solutions with current solutions, excellent individuals can enter the next generation. Mathematically, the strategy is defined as follows:

Suppose $x = (x_1, x_2, \ldots, x_D)$ is a point in the D-dimensional search space (can be regarded as a feasible solution), $x_j = [a_j, b_j]$, $j = 1,2, \ldots, D$, and its corresponding opposite point $\tilde{x} = (\tilde{x}_1, \tilde{x}_2, \ldots, \tilde{x}_D)$ can be defined as:

$$\tilde{x} = a_j + b_j - x_j \tag{21}$$

The fitness values of the current solution and the opposite solution are calculated. By comparison, the solution with the optimal fitness value is preserved.

4.2. MALO algorithm

ALO algorithm has the advantages of simple principle, fewer parameter settings and so on. It also has the problems of slower convergence speed, falling easily into the local optimum, and lower search accuracy. In order to improve the exploration and exploitation of the ALO algorithm, OBL strategy is introduced in the native ALO. The probability of convergence to the global optimum is increased. For each iteration, the position of ant Ant_i^t is obtained by Eq (19). However, there may be a possibility that Ant_i^t is opposite or near the optimal position in the search space. Therefore, after each iteration, OBL is applied to generate the opposite solution $\widetilde{Ant_i^t}$. The equation is as follows:

$$\widetilde{Ant_i^t} = ub + lb - Ant_i^t \tag{22}$$

where *ub* denotes the upper bound and *lb* denotes the lower bound.

The fitness values of the new position and the original position are compared. After the evaluation, the position with high fitness values are retained. After this process, the modification algorithm has more search attempts in each iteration [51,52].

The time complexity of MALO is given based on four factors such as the number of search agents N, the number of dimension D, the maximum number of iterations T, the cost of function F. In the initialization process, the time complexity is $O(N)$. The time complexity of sorting mechanism is $O(N \times \log N)$. The time complexity of function evaluation is $O(T \times N \times F)$. The time complexity is expressed as $O(T \times N \times D)$ for the updating the positions. The time complexity of the updating phase by the OBL is $O(T \times N \times D)$. The overall time complexity of MALO is $O(N \times (1 + \log N + T \times (F + 2D)))$.

4.3. The proposed MALO based multilevel thresholding method

The process of finding the optimal threshold is actually to find the optimal solution. However, it has high time complexity when dealing with multilevel thresholds. In order to achieve efficiency, it is entirely possible to use the modified ALO algorithm to do this. The basic steps are described as follows:

Firstly, test images in JPG format are read and histograms are obtained. The number of search agents and maximum number of iterations are initialized. MALO is implemented considering two different objective functions: Otsu and Kapur's entropy. Then, the fitness of initial population is calculated. The main loop begins with the second iteration. The updating position of ant is determined by a selected antlion by the roulette wheel and the elite. OBL strategy is applied to the obtained position of ant for generating the opposite solution. The fitness of original position and opposite position of ant are calculated and compared. The individual with high fitness value is preserved. If the fitness of ant is better than the antlion, then the position of antlion will be updated

to the position of ant. This process is repeated until the maximum number of iterations is completed. The position of elite represents the optimal thresholds. The segmentation is carried out based on the obtained thresholds. Finally, the values of the evaluation measures and the segmented images are output. The pseudo code and the flowchart of MALO algorithm based multilevel thresholding are provided in Algorithm 1 and Figure 2, respectively.

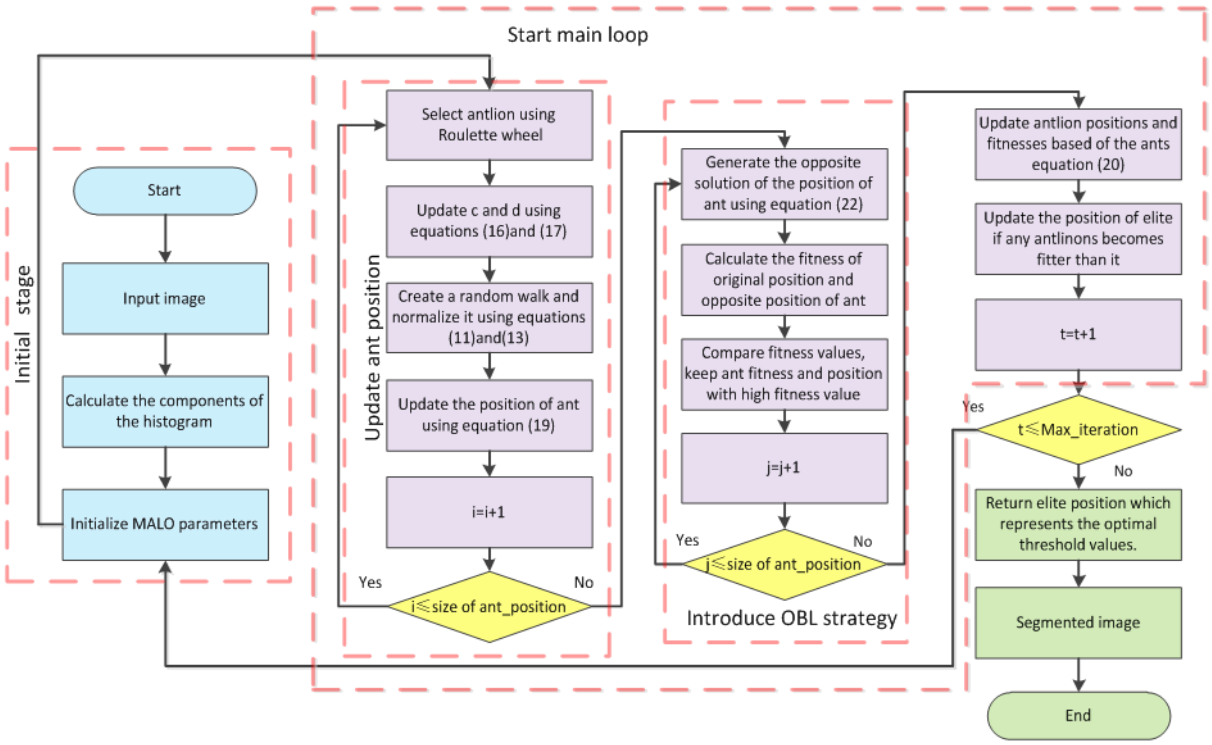

Figure 2. Flowchart of MALO algorithm based multilevel thresholding.

5. Experiments

In this section, in order to evaluate the quality of image segmentation based on MALO, a series of experiments are conducted. Firstly, Section 5.1 indicates the parameter settings of comparison algorithms, test images selected in the experiment, and operating environment. Section 5.2 introduces the metrics used to evaluate the image segmentation performance in the experiment. Section 5.3 uses IEEE CEC2017 benchmark functions to validate the effectiveness of MALO. Section 5.4 compares MALO with some traditional algorithms. The experimental data are analyzed, and the performance of image segmentation based on various algorithms is evaluated. Furthermore, Section 5.5 compares MALO with some improved algorithms. The future research is also conducted.

5.1. Experimental materials

In this paper, 10 color images are selected from the Berkeley University database [53] for performance analysis. Figure 3 shows the original test images and the corresponding histograms. All images are in JPG format with a size of 481 × 321 pixels. Each algorithm runs each image 30 times separately. The number of threshold K includes: 4, 6, 8, 10, and 12.

In order to prove the superiority of the MALO algorithm, 7 traditional algorithms and 4 improved algorithms which have been proposed and widely applied to multilevel thresholding segmentation are selected for comparisons, including SSA [17], MVO [54], DA [19], FPA [18], PSO [55], SCA [34], MABC [56], IDSA [57], WOA-TH [58], and BDE [59]. These comparison algorithms have different search strategies and mathematical equations. The maximum of iterations for all algorithms is 500 and the population size is 25. We follow the same parameters in the original papers. The main parameters of various algorithms are shown in Table 1.

All the experimental series were carried out on MATLAB R2016b, and the computer was configured as Intel(R) Core(TM) i5-4210U CPU @1.70 GHz, using Microsoft Windows 10 system.

Algorithm 1. Pseudo code of MALO algorithm based multilevel thresholding.

Input the image and calculate components of the histogram.
Initialize parameters: *SearchAgents_no* (the number of search agents), *T* (maximum number of iterations).
Calculate the fitness of initial ants and antlions;
Find the best antlions and assume it as the elite;
While $t < T$
    For each ant
        Select an antlion using Roulette wheel;
        Update *c* and *d* using Eqs **(16)** and **(17);**
        Create a random walk and normalize it using Eqs **(11)** and **(13);**
        Update the position of ant using Eq **(19)**;
    End for
    For each the position of ant
        Generate the opposite solution of the position of ant using Eq **(22)**;
        Calculate the fitness of original position and opposite position of ant;
        Compare fitness values and keep ant fitness and position with high fitness value;
    End for
    Update antlion positions and finesses based of the ants Eq **(20);**
    Update the position of elite if any antlions becomes fitter than it;
    $t = t + 1$;
End while
Return elite fitness and position, which elite position represents the optimal thresholds.
Output the values of the evaluation measures and the segmented images.

Table 1. Parameters for the compared algorithms.

Algorithm	Parameters	Value
SSA	Balance coefficient c_1	[0,2]
	Random number c_2, c_3	[0,1]
	Switch possibility	0.5
MVO	Wormhole Existence Probability	[0.2,1]
	Travelling Distance Rate	[0,1]
	Random number r_1, r_2, r_3	[0,1]
DA	Inertial weight ω	[0.5,0.9]
	Seperation weight	[0,0.2]
	Alignment weight	[0,0.2]
	Cohesion weight	[0,0.2]
	Food factor	[0,2]
	Enemy factor	[0,0.1]
FPA	Switch possibility	0.4
	Lévy constant β	1.5
PSO	Maximum inertia weight	0.9
	Minimum inertia weight	0.4
	Learning factors c_1, c_2	2
	Maximum velocity	+120
	Minimum velocity	−120
SCA	Movement direction r_1	[0,2]
	Movement distance r_2	[0,2π]
	Random weight r_3	[0,2]
	Random number r_4	[0,1]
	Switch possibility	0.5
ALO	Switch possibility	0.5
MABC	Random number r	[0,1]
IDSA	Random number r	[0,1]
WOA-TH	Parameter a	[0,2]
	Constant b	1
	Random number l	[−1,1]
	Constant a_0	13
	Initial value G_0	40
BDE	Number of objectives	1
	Number of constraints	0
	Number of decision variables	4
	Scaling factor	0.5
	Crossover probability	0.2

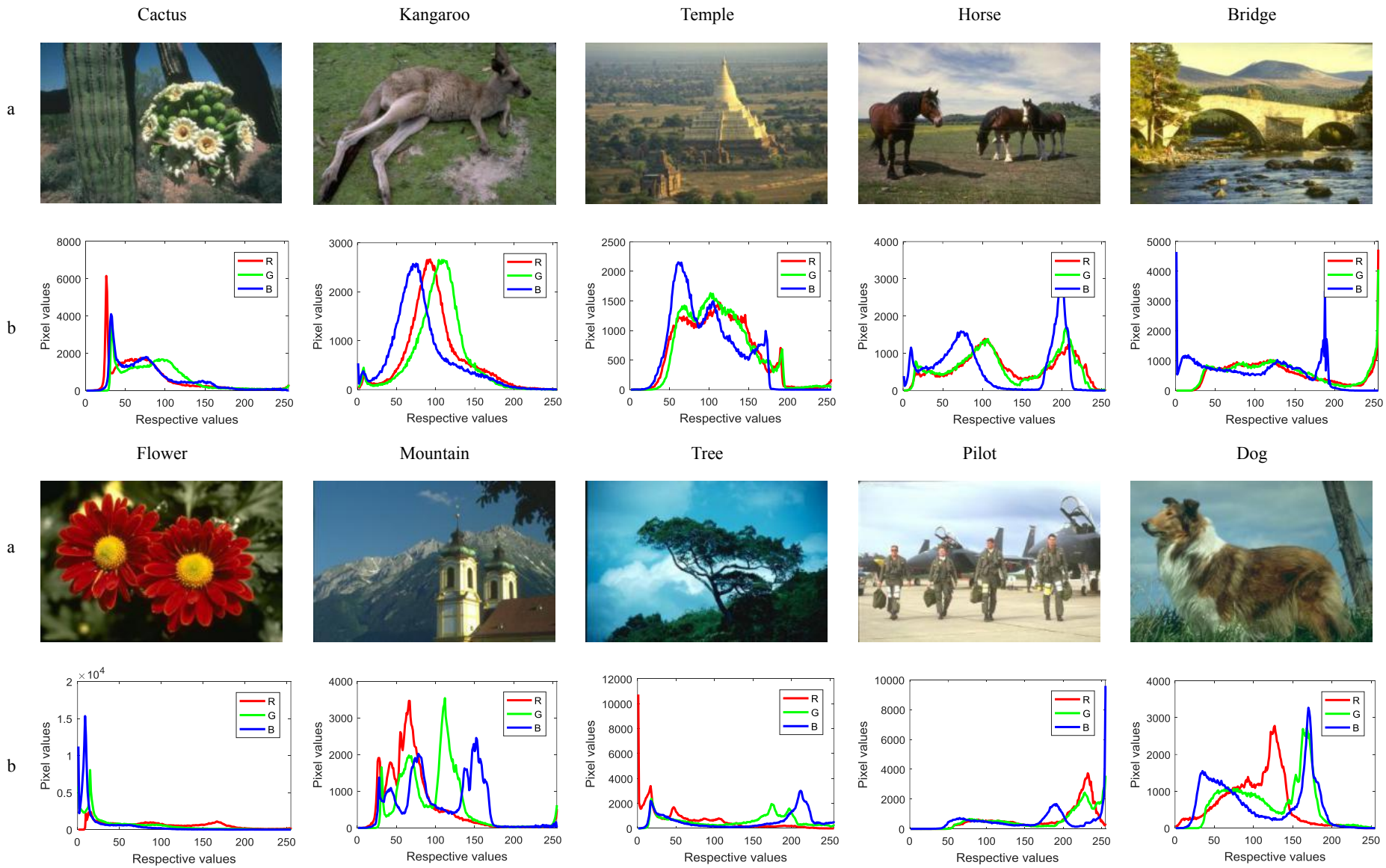

Figure 3. Original test images and histograms. (Line a represent images; line b represent histograms.)

5.2. Evaluation measurements

This paper evaluates the quality of image segmentation from the following five aspects：

1) Fitness value. Since Otsu and Kapur's entropy methods are maximization problem, the fitness values are expected to be as large as possible. The optimal fitness values show that the algorithm has high accuracy and convergence performance.

2) PSNR. It is an objective evaluation measure based on pixel error. A higher PSNR value indicates that the quality of the distorted image is better. However, it is based on the error between corresponding pixels and does not consider the visual characteristics of human eyes. Its calculation equation is as follows:

$$\text{PSNR} = 10\log_{10}\frac{L^2}{MSE}(db) \tag{23}$$

where L represents the scale range of the image. For an 8-bit image, $L = 255$. MSE is the mean square error between the original image and the processed image.

$$MSE = \frac{\sum_{m=1}^{M}\sum_{n=1}^{N}\left[R(m,n) - I(m,n)\right]^2}{M \times N} \tag{24}$$

where $M \times N$ is the size of the image, $R(m,n)$ represents the gray value of coordinates at the reference image (m, n), and $I(m,n)$ represents the gray value of coordinates at the distorted image (m, n).

3) SSIM. It is an objective evaluation measure based on structural similarity. It measures the image similarity from brightness, contrast, and structure. SSIM value range is [0, 1]. If the value is closer to 1, the image distortion is smaller. It is defined as follows：

$$\text{SSIM}(R, I) = \frac{(2\mu_R\mu_I + C_1)(2\sigma_{RI} + C_2)}{(\mu_R^2 + \mu_I^2 + C_1)(\sigma_R^2 + \sigma_I^2 + C_2)} \tag{25}$$

where U_R and U_I are the average gray values of the original image R and the segmented image I, respectively. σ_R^2 and σ_I^2 represent the variance of image R and image I, respectively. σ_{RI} is the covariance of image R and image I. $C_1 = (0.01L)^2$, $C_2 = (0.03L)^2$.

4) FSIM. Based on SSIM, researchers have proposed a new evaluation measure, namely feature similarity algorithm (FSIM). We use two complementary features of phase congruency (PC) and gradient magnitude (GM) to calculate FSIM.

$$\text{FSIM} = \frac{\sum_{x\in\Omega} S_L(x) \times PC_m(x)}{\sum_{x\in\Omega} PC_m(x)} \tag{26}$$

where Ω is the pixel field of the entire image, $S_L(x)$ represents the similarity value of each position x,

and $PC_m(x)$ denotes the phase consistency measure.

$$S_L(x) = \left[S_{PC}(x)\right]^{\alpha} \times \left[S_G(x)\right]^{\beta} \tag{27}$$

$$PC_m(x) = max\left(PC_1(x), PC_2(x)\right) \tag{28}$$

where $S_{PC}(x)$ is the similarity measure of phase consistency, $S_G(x)$ represents the similarity measure of gradient magnitude, and α, β are both constants.

$$S_{PC}(x) = \frac{2PC_1(x) \times PC_2(x) + T_1}{PC_1^2(x) \times PC_2^2(x) + T_1} \tag{29}$$

$$S_G(x) = \frac{2G_1(x) \times G_2(x) + T_2}{G_1^2(x) \times G_2^2(x) + T_2} \tag{30}$$

where T_1 and T_2 are positive constants.

5) Computational time. The smaller the value, the faster the algorithm execution speed.

5.3. Comparison with traditional algorithms on IEEE CEC2017 benchmark functions

In this subsection, 29 IEEE CEC2017 benchmark functions are chosen to check the efficiency of algorithms. We skip "F2" of IEEE CEC2017 because of its unstable behavior. These functions are divided into four groups: unimodal (F1–F3), multimodal (F4–F10), hybrid (F11–F20), and composition (F21–F30). Furthermore, the relevant composition, dimension, range limitation and optimal position of 29 functions can be found in [43]. Meanwhile, all experiments are conducted 30 times.

In MALO, the OBL strategy can developed more in the later search period. Compared with the native ALO, it has excellent exploration and exploitation. For the OBL strategy, putting it into ALO as a strategy can greatly improve the convergence and high efficiency. The performance of algorithms is evaluated according to the mean value (Mean) and standard deviation (Std). The stability of each model is evaluated by Std value. Meanwhile, the best results has been highlighted in boldface in Table 2. From the table above, we can observe that MALO based method gives the satisfied results in general. For example, in the unimodal and multimodal functions, the proposed method gives better results in 10 out of 18 cases (9 functions and 2 indexes). In terms of hybrid functions, the MALO based method outperforms in 12 out of 20 cases (10 functions and 2 indexes) for others. In the composition functions, the proposed method gives better results in 10 out of 20 cases (10 functions and 2 indexes). All the other algorithms show a certain difference with MALO based method. The experimental results above are effectively proved the superior performance of proposed method. The ability to avoid local optimization has enhanced. Thus, it can be said that the proposed method in this paper is more effective than competitors in 29 benchmark functions, so this paper combines MALO with multilevel thresholding segmentation method to improve the image segmentation accuracy.

Table 2. Comparison of the mean and standard deviation of fitness values obtained.

F		SSA	MVO	DA	FPA	PSO	SCA	ALO	MALO
F1	Mean	2.7525 × 10^3	2.0775 × 10^4	5.3030 × 10^7	9.4246 × 10^7	2.3768 × 10^3	1.1165 × 10^9	1.6205 × 10^3	**2.2691 × 10^2**
	Std	3.1853 × 10^3	1.0204 × 10^4	1.3048 × 10^8	1.6194 × 10^8	3.3853 × 10^3	2.6690 × 10^8	1.6927 × 10^3	**7.5223 × 10^2**
F3	Mean	**3.0002 × 10^2**	3.0015 × 10^2	3.3792 × 10^3	5.6230 × 10^3	3.0009 × 10^2	3.0174 × 10^3	4.5012 × 10^2	4.4652 × 10^2
	Std	8.4151 × 10^{-2}	**7.5858 × 10^{-2}**	3.5353 × 10^3	3.7208 × 10^3	7.7137 × 10^{-2}	1.6524 × 10^3	3.7837 × 10^2	3.1829 × 10^2
F4	Mean	4.0989 × 10^2	4.0702 × 10^2	4.2856 × 10^2	4.6977 × 10^2	4.0507 × 10^2	4.6709 × 10^2	4.1395 × 10^2	**4.0394 × 10^2**
	Std	16.908	9.3281	29.903	61.297	**1.2334**	30.876	22.338	12.248
F5	Mean	5.2912 × 10^2	5.2264 × 10^2	5.1732 × 10^2	5.6206 × 10^2	5.4292 × 10^2	5.5799 × 10^2	5.2180 × 10^2	**5.1692 × 10^2**
	Std	12.497	1.1788 × 10	8.4145	21.327	14.890	6.6091	13.640	**2.8811**
F6	Mean	6.1533 × 10^2	6.0237 × 10^2	**6.0125 × 10^2**	6.3945 × 10^2	6.1021 × 10^2	6.2361 × 10^2	6.1562 × 10^2	6.7956 × 10^2
	Std	8.9433	3.1079	**1.4272**	16.075	8.8947	5.4162	8.8988	10.159
F7	Mean	7.4500 × 10^2	7.3257 × 10^2	7.3766 × 10^2	7.9322 × 10^2	7.3056 × 10^2	7.8595 × 10^2	7.5048 × 10^2	**7.2403 × 10^2**
	Std	15.007	12.483	14.458	26.384	12.387	10.193	26.572	**2.3596**
F8	Mean	8.2630 × 10^2	8.2696 × 10^2	8.1554 × 10^2	8.4529 × 10^2	8.2131 × 10^2	8.4537 × 10^2	8.2771× 10^2	**8.1001 × 10^2**
	Std	11.690	12.498	**7.2712**	16.236	7.9025	8.7128	14.163	9.4471
F9	Mean	1.0897 × 10^3	**9.0116 × 10^2**	9.2457 × 10^2	1.7066 × 10^3	9.6607 × 10^2	1.0671 × 10^3	1.1272 × 10^3	1.0417 × 10^3
	Std	2.5134 × 10^2	**2.8801**	51.037	6.1484 × 10^2	1.1193 × 10^2	81.732	2.2796 × 10^2	1.8741 × 10^2
F10	Mean	1.8446 × 10^3	1.7723 × 10^3	1.7989 × 10^3	2.1907 × 10^3	1.9995 × 10^3	2.5054 × 10^3	2.0639 × 10^3	**1.2226 × 10^3**
	Std	2.8235 × 10^2	2.8547 × 10^2	3.4047 × 10^2	3.9008 × 10^2	2.9524 × 10^2	2.0358 × 10^2	3.1110 × 10^2	**1.7148 × 10^2**
F11	Mean	1.1840 × 10^3	**1.1325 × 10^3**	1.2913 × 10^3	1.2604 × 10^3	1.1388 × 10^3	1.2494 × 10^3	1.2125 × 10^3	9.3895 × 10^4
	Std	71.184	27.254	8.0087 × 10^2	1.1285 × 10^2	2.7432 × 10^5	76.249	74.386	**24.745**
F12	Mean	3.1659 × 10^6	1.9237 × 10^6	8.5333 × 10^5	5.3131 × 10^6	2.8460 × 10^9	3.6304 × 10^7	2.9647 × 10^6	**2.2571 × 10^4**
	Std	3.9918 × 10^6	2.4011 × 10^6	1.0164 × 10^6	5.2872 × 10^6	1.4432 × 10^9	4.6673 × 10^7	3.6635 × 10^6	**3.1055 × 10^4**

Continued on next page

F		SSA	MVO	DA	FPA	PSO	SCA	ALO	MALO
F13	Mean	1.7372 × 10^4	1.2349 × 10^4	1.6552 × 10^4	2.3449 × 10^4	3.2613 × 10^8	8.9513 × 10^4	1.3896 × 10^4	**1.1517 × 10^4**
	Std	1.2611 × 10^4	9.7419 × 10^3	9.0887 × 10^3	1.8794 × 10^4	2.7709 × 10^8	8.0007 × 10^4	1.2201 × 10^4	**7.8833 × 10^3**
F14	Mean	3.3621 × 10^3	3.0338 × 10^3	4.8484 × 10^3	2.8067 × 10^3	2.8688 × 10^3	2.3311 × 10^3	2.6070 × 10^3	**2.3278 × 10^3**
	Std	2.7150 × 10^3	2.3148 × 10^3	1.8854 × 10^3	1.4364 × 10^3	2.1263 × 10^3	**1.0895 × 10^3**	1.6260 × 10^3	1.2880 × 10^3
F15	Mean	6.2001 × 10^3	3.3924 × 10^3	6.4284 × 10^3	9.6586 × 10^3	3.9125 × 10^3	3.7996 × 10^3	1.3375 × 10^4	**3.0564 × 10^3**
	Std	4.2086 × 10^3	3.5797 × 10^3	5.0026 × 10^3	7.7162 × 10^3	3.7024 × 10^3	2.3791 × 10^3	1.0871 × 10^4	**2.1255 × 10^3**
F16	Mean	1.8063 × 10^3	1.8309 × 10^3	**1.7338 × 10^3**	1.9840 × 10^3	1.8428 × 10^3	1.8126 × 10^3	1.8928 × 10^3	1.8066 × 10^3
	Std	1.4760 × 10^2	1.6725 × 10^2	1.2125 × 10^2	1.4716 × 10^2	1.2492 × 10^2	**80.085**	1.6074 × 10^2	1.0356 × 10^2
F17	Mean	1.7831 × 10^3	1.7871 × 10^3	1.7693 × 10^3	1.8044 × 10^3	1.7796 × 10^3	1.7897 × 10^3	1.7795 × 10^3	**1.7359 × 10^3**
	Std	38.227	56.931	33.562	52.636	59.130	**14.372**	39.757	34.260
F18	Mean	1.9046 × 10^4	1.7527 × 10^4	2.4433 × 10^4	**1.5703 × 10^4**	1.6595 × 10^4	4.2187 × 10^5	1.6102 × 10^4	1.6102 × 10^4
	Std	1.3350 × 10^4	**1.1493 × 10^4**	1.5706 × 10^4	1.2231 × 10^4	1.3320 × 10^4	4.6787 × 10^5	1.3045 × 10^4	1.2885 × 10^4
F19	Mean	9.3321 × 10^3	4.8206 × 10^3	1.1236 × 10^4	9.2778 × 10^4	5.1293 × 10^3	1.0034 × 10^4	1.6927 × 10^4	**1.9544 × 10^3**
	Std	7.1553 × 10^3	4.0080 × 10^3	6.8870 × 10^3	2.0401 × 10^5	3.8240 × 10^3	8.8662 × 10^3	1.2359 × 10^4	**3.1306 × 10^3**
F20	Mean	2.1580 × 10^3	2.1181 × 10^3	2.1072 × 10^3	2.1974 × 10^3	2.1351 × 10^3	2.1393 × 10^3	2.1520 × 10^3	**2.1017 × 10^3**
	Std	77.357	71.982	59.164	81.489	81.620	**37.232**	76.695	1.1244 × 10^2
F21	Mean	**2.2892 × 10^3**	2.3067 × 10^3	2.3146 × 10^3	2.3260 × 10^3	2.3033 × 10^3	2.2951 × 10^3	2.3181 × 10^3	2.2919 × 10^3
	Std	58.652	43.950	23.354	56.359	69.965	67.337	23.092	**23.025**
F22	Mean	2.3032 × 10^3	2.4325 × 10^3	2.3387 × 10^3	2.3737 × 10^3	2.3168 × 10^3	2.3923 × 10^3	2.3019 × 10^3	**2.2108 × 10^3**
	Std	**1.5330**	4.0570 × 10^2	1.5916 × 10^2	3.0758 × 10^2	86.302	36.970	14.139	4.3619
F23	Mean	2.6246 × 10^3	**2.6213 × 10^3**	2.6263 × 10^3	2.6544 × 10^3	2.6993 × 10^3	2.6630 × 10^3	2.6330 × 10^3	2.6235 × 10^3
	Std	9.4651	**8.4456**	11.398	27.680	38.621	9.4154	13.016	8.6164

Continued on next page

F		SSA	MVO	DA	FPA	PSO	SCA	ALO	MALO
F24	Mean	2.7448 × 10^3	2.7399E+03	2.7422E+03	2.7726E+03	2.7821E+03	2.7773E+03	2.7541E+03	**2.7242E+03**
	Std	48.315	45.915	47.575	55.733	1.1838 × 10^2	59.112	13.296	**10.259**
F25	Mean	2.9316 × 10^3	2.9322 × 10^3	2.9355 × 10^3	2.9755 × 10^3	**2.9227 × 10^3**	2.9816 × 10^3	2.9352 × 10^3	2.9316 × 10^3
	Std	30.687	28.163	23.579	53.181	**23.221**	24.991	28.272	2.7704 × 10^2
F26	Mean	**2.9852 × 10^3**	3.0412 × 10^3	3.1910 × 10^3	3.5113 × 10^3	3.2078 × 10^3	3.1238 × 10^3	3.0689 × 10^3	3.0597 × 10^3
	Std	2.7007 × 10^2	3.8042 × 10^2	3.9782 × 10^2	4.9123 × 10^2	5.0084 × 10^2	**37.746**	2.7801 × 10^2	2.5490 × 10^2
F27	Mean	3.0942 × 10^3	3.0936 × 10^3	3.0975 × 10^3	3.1538 × 10^3	3.1493 × 10^3	3.1084 × 10^3	3.1028 × 10^3	**3.0346 × 10^3**
	Std	3.6648	3.4486	6.0913	55.897	67.675	4.4917	15.597	**1.4249**
F28	Mean	3.3187 × 10^3	3.3510 × 10^3	3.3579 × 10^3	3.4196 × 10^3	3.2028 × 10^3	3.3398 × 10^3	3.3863 × 10^3	**3.1170 × 10^3**
	Std	1.6379 × 10^2	1.3529 × 10^2	95.702	1.6486 × 10^2	**78.068**	90.179	1.3401 × 10^2	1.0508 × 10^2
F29	Mean	3.2573 × 10^3	3.2282 × 10^3	3.2212 × 10^3	3.4234 × 10^3	3.2563 × 10^3	3.2629 × 10^3	3.2707 × 10^3	**3.1694 × 10^3**
	Std	81.947	83.366	55.368	1.3273 × 10^2	82.282	33.745	94.979	**22.526**
F30	Mean	5.4626 × 10^5	5.5507 × 10^5	1.0112 × 10^6	2.2409 × 10^6	6.8210 × 10^4	1.7827 × 10^6	7.0103 × 10^5	**1.5116 × 10^4**
	Std	5.8213 × 10^5	6.5747 × 10^5	1.3632 × 10^6	2.9983 × 10^6	**6.4354 × 10^4**	1.3111 × 10^6	2.1161 × 10^6	7.2776 × 10^4

5.4. Comparison with traditional algorithms on Berkeley images

The fitness value can be used as an index to evaluate the performance of segmentation method. All the experiments are conducted 30 times on 10 color images. Tables 3 and 4 respectively show average fitness values using Otsu and Kapur's entropy compared with other algorithms. In every line, the maximum is in bold. From these tables, it can be seen that MALO algorithm finds the maximum fitness values more times than other algorithms. However, the same objective function value obtained by several algorithms also occasionally occurs when the threshold value is small (such as K = 4, 6, and 8). Overall, the OBL strategy can improve the calculation accuracy of ALO algorithm, which helps to find the global optimal solution and improve the overall performance.

In order to make the experimental data more intuitive, the following experiments are conducted. The relevant convergence curve and boxplot are drawn. As shown in Figure A1 and A2, the evolution curve reflects the convergence speed and the accuracy of the algorithm, thus reflecting the overall performance of the algorithm. It can be seen from the convergence curve that the MALO algorithm can obtain the approximate optimal solution, which further improves the overall performance. For

Table A2(d),(h), MALO algorithm and DA algorithm eventually approach the same function value. But for the rest of graphs, it is clear that the MALO algorithm is superior to other algorithms in the optimization process. MALO algorithm can reach the maximum fitness value at nearly the 100th iteration, which is earlier than other algorithms. This phenomenon indicates that the convergence rate of algorithm is improved. On the whole, it also proves that by introducing the OBL strategy, the stability of the algorithm is enhanced. As shown in Figures 4 and 5, the boxplot can effectively reflect the stability of the algorithm. Taking the two images of cactus and kangaroo as examples, it can be seen that the boxplot of MALO algorithm has the most flat shape, the highest position, and no bad points. This shows that the MALO algorithm has the highest stability compared with other algorithms by analysis of the 30 fitness values obtained.

Table 3. Comparison of fitness values obtained with each algorithm for Otsu.

Image	K	SSA	MVO	DA	FPA	PSO	SCA	ALO	MALO
	4	**2126.2412**	**2126.2412**	**2126.2412**	2084.2192	2126.2085	2091.2043	2126.1077	**2126.2412**
	6	2188.8026	2188.7881	2188.7749	2152.9126	2180.5976	2151.3710	2188.6529	**2188.8076**
Cactus	8	2213.1588	2213.1207	2210.6763	2185.1975	2206.7101	2177.4155	2212.8736	**2213.2108**
	10	2224.0745	2224.9921	2224.4972	2202.9660	2224.8409	2205.3385	2223.8535	**2225.0378**
	12	2228.0349	2231.4043	2227.1859	2208.4757	2230.3736	2209.0205	2230.9917	**2231.8810**
	4	**1114.7964**	**1114.7964**	**1114.7964**	1088.7665	1114.7783	1088.6203	1114.7451	**1114.7964**
	6	1164.7339	1164.7235	1162.2148	1131.7231	1157.9995	1142.5799	1164.5055	**1164.7463**
Kangaroo	8	1186.9998	1187.2317	1186.4981	1164.0753	1181.4079	1157.1404	1187.0901	**1187.3921**
	10	1195.5800	1198.8061	1198.1305	1175.6658	1195.7200	1172.3154	1197.6616	**1199.0721**
	12	1201.3621	1204.3553	1204.0964	1189.4752	1203.7897	1186.9269	1204.8168	**1205.6190**
	4	1510.8080	1511.3099	**1511.3110**	1481.4555	1511.2952	1484.9151	1511.1720	**1511.3110**
	6	1562.1584	1551.2497	1562.1657	1539.3204	1547.2460	1528.3151	1562.0323	**1562.1677**
Temple	8	1575.4345	1581.9379	1580.1512	1558.9731	1577.2711	1552.2760	1578.5870	**1582.0010**
	10	1585.0462	1589.3769	1588.9537	1566.9471	1583.4601	1562.6224	1589.3855	**1590.0709**
	12	1593.4902	1592.3625	1594.7102	1577.6113	1589.2313	1577.5018	1595.2350	**1596.7043**
	4	**2319.2628**	**2319.2628**	**2319.2628**	2300.8905	**2319.2628**	2305.0308	2319.2088	**2319.2628**
	6	2373.7148	2373.9784	2373.9666	2349.7530	2366.7255	2348.8170	2373.7751	**2374.0062**
Flower	8	2398.3260	2397.7703	2398.6865	2373.7415	2393.6744	2378.1142	2398.0974	**2398.7056**
	10	2408.6487	2409.1083	2410.1377	2392.7685	2409.5320	2393.4470	2409.9581	**2410.1748**
	12	2415.5456	2416.1915	2413.2197	2401.7458	2413.6013	2402.8505	2416.6995	**2417.4773**
	4	**1922.6304**	**1922.6304**	**1922.6304**	1880.8725	**1922.6304**	1899.0075	1922.5604	**1922.6304**
	6	1966.3537	1969.5924	1969.5227	1950.3434	1964.7413	1937.2954	1969.3259	**1969.6134**
Mountain	8	1987.6882	1987.6512	1987.6006	1971.0006	1982.4353	1963.1189	1987.3940	**1989.0684**
	10	1998.2296	1998.3989	1999.2217	1976.2590	1995.3262	1980.4772	1998.6023	**1999.5736**
	12	2002.3212	2003.5176	2003.4479	1991.7908	2002.3326	1987.1898	2003.1927	**2004.4332**
	4	**4836.5287**	4836.5254	**4836.5287**	4811.7023	4836.5184	4799.5909	4836.4226	**4836.5287**
	6	**4910.3426**	4910.3170	4910.3328	4881.3483	4899.1851	4889.6357	4909.9888	4910.3389
Tree	8	4938.5519	4938.7280	4939.0548	4895.7628	4932.5126	4897.8287	4939.0439	**4939.2738**
	10	4954.4191	4954.3250	4954.3494	4931.0184	4950.5741	4925.6878	4953.6297	**4954.7408**
	12	4961.5040	4962.0370	4961.7003	4947.5680	4958.4948	4933.2448	4961.9255	**4962.8681**

Continued on next page

Image	K	SSA	MVO	DA	FPA	PSO	SCA	ALO	MALO
	4	**4169.9500**	**4169.9500**	4169.9475	4146.0648	**4169.9500**	4125.8875	4169.9152	**4169.9500**
	6	4223.2790	4226.2869	4226.2925	4206.4679	4226.2960	4184.3739	4226.1384	**4226.2981**
Horse	8	4251.0736	4247.9571	4250.7202	4224.2255	4242.3477	4224.8735	4251.0627	**4251.0806**
	10	4264.1067	4264.0484	4263.6881	4245.5168	4263.0609	4242.4543	4263.8776	**4264.5464**
	12	4271.0552	4270.2470	4270.4589	4253.0366	4270.9270	4255.1561	4269.9287	**4272.7303**
	4	**4386.0155**	**4386.0155**	**4386.0155**	4348.0212	**4386.0155**	4364.6402	4385.8679	**4386.0155**
	6	4448.8450	4456.6582	**4456.6941**	4430.7839	4456.6543	4416.6522	4448.6228	**4456.6941**
Bridge	8	4483.9318	4476.1230	4481.9799	4459.7426	4480.7550	4436.7087	4480.4869	**4484.0957**
	10	4495.8304	4494.1137	4497.7496	4475.7876	4494.2483	4472.8251	4497.6619	**4498.1770**
	12	4505.0626	4504.6934	4502.9179	4488.9690	4504.8794	4485.6536	4504.6902	**4506.5159**
	4	**3854.8970**	**3854.8970**	**3854.8970**	3838.0151	3854.8930	3807.6575	3854.8127	**3854.8970**
	6	**3902.7853**	3896.5334	3902.7747	3884.5667	3902.7796	3869.1994	3902.6187	3902.7731
Pilot	8	3917.0447	3917.7421	3920.6198	3892.5037	3918.0121	3895.6690	3920.4228	**3923.5580**
	10	3931.0115	3928.4714	3933.5071	3915.8877	3931.1832	3904.4969	3932.5873	**3934.2915**
	12	3937.8965	3936.9459	3936.6517	3916.5100	3935.4087	3916.0317	3939.2200	**3940.3098**
	4	**2249.9855**	2249.9839	**2249.9855**	2231.2675	**2249.9855**	2233.1946	2249.9484	**2249.9855**
	6	2299.7269	2299.6899	2298.6466	2270.5848	2287.9683	2277.7186	2299.5470	**2299.7446**
Dog	8	2320.5275	2317.0263	2320.4939	2297.8192	2303.3155	2296.9113	2320.2281	**2320.5319**
	10	2326.4485	2329.6067	2330.9585	2311.9971	2328.1692	2306.4227	2330.4593	**2330.9965**
	12	2334.7496	2336.2099	2334.3909	2323.5986	2332.0819	2320.2905	2335.7878	**2337.4348**

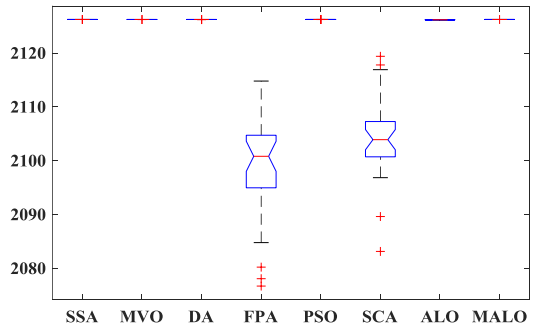

(a) Cactus (K = 4)

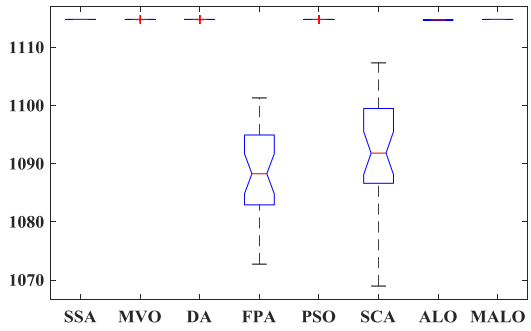

(b) Kangaroo (K = 4)

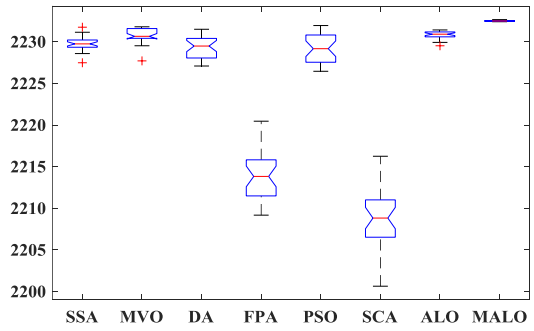

(a) Cactus (K = 12)

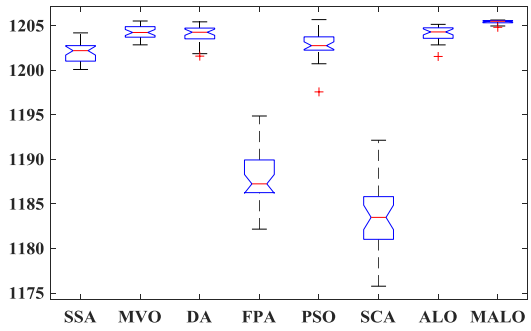

(b) Kangaroo (K = 12)

Figure 4. Boxplots for fitness values using Otsu.

Table 4. Comparison of fitness values obtained with each algorithm for Kapur's entropy.

Image	K	SSA	MVO	DA	FPA	PSO	SCA	ALO	MALO
	4	**18.5843**	**18.5843**	**18.5843**	18.3930	18.5829	18.4259	18.5832	**18.5843**
	6	23.8329	23.8233	23.8386	23.2412	23.8389	23.2857	23.8364	**23.8420**
Cactus	8	28.4940	28.3247	28.5120	27.0680	28.4911	27.3938	28.4814	**28.5198**
	10	32.6224	32.0489	32.7875	30.4517	32.8282	30.7148	32.7883	**32.8463**
	12	36.7255	35.3654	36.6688	34.7456	36.7983	34.2975	36.6721	**36.8450**
	4	**18.9363**	18.9353	18.9361	18.6549	18.9352	18.7771	18.9350	**18.9363**
	6	24.4683	24.4414	24.4720	23.6425	24.4648	24.0457	24.4563	**24.4753**
Kangaroo	8	29.3790	29.2133	29.3699	28.7933	29.4014	28.2712	29.4026	**29.4202**
	10	33.8064	33.4514	33.8602	32.6267	33.1534	32.0603	33.8653	**33.9054**
	12	37.8707	37.1153	37.9876	36.2125	38.0001	35.4540	37.9065	**38.0410**
	4	17.8159	17.8201	17.8061	17.4725	17.8046	17.5013	17.8195	**17.8204**
	6	**22.9388**	22.7544	**22.9388**	22.2007	22.8940	22.0680	22.9246	**22.9388**
Temple	8	27.5032	27.2493	27.4436	25.9640	27.4909	25.5465	27.5208	**27.5351**
	10	31.6211	30.6718	31.6425	29.5279	31.6160	28.9053	31.6706	**31.7574**
	12	34.2789	33.0925	35.3472	31.7622	34.7704	32.2631	35.3818	**35.6116**
	4	18.7000	18.6993	18.7000	18.4447	18.6996	18.4765	18.6980	**18.7005**
	6	24.0481	24.0186	24.0485	23.6039	24.0429	23.3247	24.0441	**24.0511**
Flower	8	28.7647	28.6438	28.7955	27.6104	28.7721	27.7280	28.7727	**28.8057**
	10	33.0270	32.9200	33.1672	31.2963	33.1582	31.3512	33.1673	**33.1976**
	12	36.8699	35.9637	37.1214	34.8362	37.0372	34.9773	36.9291	**37.1549**
	4	17.7231	17.7035	17.7213	17.5421	17.7372	17.4362	**17.7390**	17.7213
	6	**23.1283**	23.0802	23.0902	22.5402	23.1001	22.4117	23.1173	23.1119
Mountain	8	27.9637	27.6405	27.9315	26.6905	27.9354	26.4147	27.9302	**27.9679**
	10	32.1404	31.9221	32.3451	30.9813	32.2561	30.0080	32.3415	**32.4426**
	12	36.3399	34.9350	36.3823	34.0005	35.6920	33.6967	36.1384	**36.4707**
	4	**18.9965**	18.9962	**18.9965**	18.8465	18.9961	18.8254	18.9953	**18.9965**
	6	24.3933	24.4095	24.4100	23.8731	24.3889	23.4245	24.4083	**24.4149**
Tree	8	29.2846	28.9004	29.2918	27.8265	29.2753	27.6207	29.2581	**29.2936**
	10	33.5397	33.0809	33.6613	31.4879	33.6439	31.7828	33.5491	**33.6785**
	12	37.3776	36.7041	37.4570	35.2858	37.5764	34.8717	37.5111	**37.6312**
	4	18.6614	18.6259	18.6230	18.3914	18.6252	18.5251	18.6614	**18.6619**
	6	24.0609	23.8743	24.0802	23.2431	24.0604	22.8699	24.0675	**24.0806**
Horse	8	28.8403	28.5613	28.8907	27.9542	28.8416	27.6730	28.8914	**28.8992**
	10	33.2142	32.3696	33.2125	31.1950	33.2741	30.7256	33.2480	**33.3135**
	12	36.8467	35.6548	37.0718	34.9857	37.0695	33.8890	37.1782	**37.3216**
	4	18.1906	18.1436	18.1902	18.0033	18.1903	18.0580	18.1903	**18.1907**
	6	23.5631	23.5510	23.5679	22.8880	23.5610	22.8246	23.5649	**23.5682**
Bridge	8	28.2604	27.9986	28.2930	27.0830	28.2859	26.7516	28.2786	**28.3023**
	10	32.5876	32.3366	32.5480	30.9047	32.5740	30.5593	32.5281	**32.6189**
	12	36.0703	35.4806	36.4991	33.5753	36.4588	33.0662	36.4400	**36.5351**

Continued on next page

Image	K	SSA	MVO	DA	FPA	PSO	SCA	ALO	MALO
	4	**17.9368**	17.9352	17.9362	17.6027	17.9362	17.7058	17.9355	17.9168
	6	23.0182	22.9648	23.0443	21.9322	23.0365	21.8927	23.0025	**23.0447**
Pilot	8	27.6539	27.4187	27.6678	26.2966	27.6452	25.7373	27.6307	**27.6723**
	10	31.6001	30.3305	31.7457	30.5445	31.7701	29.3977	31.7568	**31.8639**
	12	35.3121	34.3457	35.4310	32.7740	35.6276	31.7852	35.5945	**35.7388**
	4	18.5258	18.5246	18.4850	18.2690	18.5254	18.2825	18.5244	**18.5261**
	6	23.6922	23.6586	23.7386	22.7559	23.7121	22.7675	23.7319	**23.7420**
Dog	8	28.3767	28.0194	28.3553	27.0852	28.3862	26.7027	28.3751	**28.4079**
	10	32.4951	31.5916	32.6709	31.2171	32.6231	29.8432	32.6604	**32.6944**
	12	36.4563	36.2405	36.3900	34.1968	35.8826	33.0948	36.5074	**36.6079**

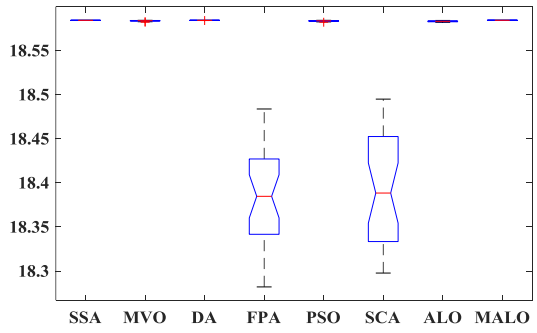

(a) Cactus (K = 4)

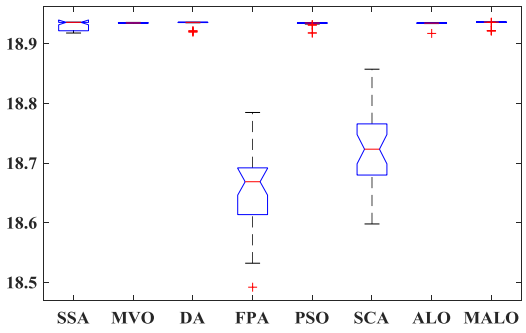

(b) Kangaroo (K = 4)

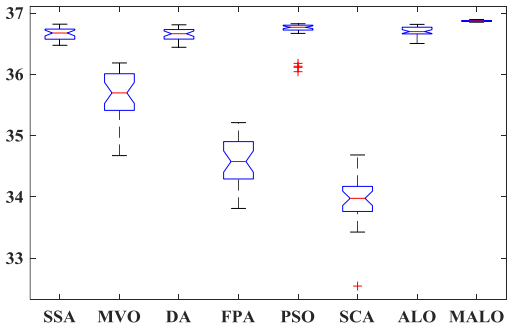

(a) Cactus (K = 12)

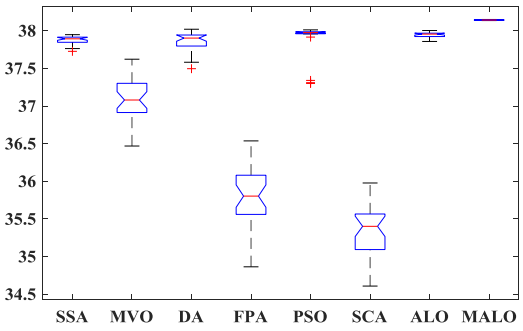

(b) Kangaroo (K = 12)

Figure 5. Boxplots for fitness values using Kapur's entropy.

Tables A2 and A3 show PSNR values of Otsu and Kapur's entropy respectively. When the PSNR value is larger, the distortion of the segmented image is smaller. Through the data, it can be seen vertically that the PSNR value of high threshold is larger than that of low threshold. We see horizontally that the PSNR value of MALO algorithm is larger than other algorithms in most cases, especially at high threshold level. Tables A4 and A5 show SSIM values of Otsu and Kapur's entropy, respectively. Tables A6 and A7 show FSIM values of Otsu and Kapur's entropy, respectively. When the values of SSIM value and FSIM value are closer to 1, the images before and after segmentation are more similar and the segmentation effect is better. Comparing SSIM value and FSIM value, MALO algorithm is larger and closer to 1 than other algorithms. The maximum value is marked in bold. Most of the

evaluation metrics obtained by MALO algorithm are optimal. The modified algorithm makes the image segmentation effect better.

Table 5. The average computational time (in second) of each algorithm using Otsu.

Image	K	SSA	MVO	DA	FPA	PSO	SCA	ALO	MALO
	4	0.4100	0.8700	1.8700	0.6900	0.7700	0.7100	1.4050	1.7200
	6	0.2500	0.7000	1.4900	0.6800	0.6700	0.6500	1.8700	2.1455
Cactus	8	0.2810	0.7800	1.5200	0.6800	0.7200	0.6800	2.3850	2.6000
	10	0.3200	0.7800	1.5600	0.7300	0.7600	0.7100	2.9545	3.2550
	12	0.3400	1.0600	1.6890	0.8630	0.9000	0.8400	4.8515	4.3270
	4	0.5050	0.8100	1.8420	0.6700	0.7300	0.9580	1.4200	1.5505
	6	0.2690	0.7300	1.5200	0.6800	0.7600	0.6500	1.9600	2.1995
Kangaroo	8	0.3100	0.8300	1.6410	0.7010	0.7500	0.7400	2.4345	2.7155
	10	0.3400	0.8500	1.6000	0.7800	0.8200	0.7400	3.0750	3.3250
	12	0.3700	0.8400	1.6000	0.7800	0.8300	0.7900	3.7580	3.8305
	4	0.3700	0.8540	1.9250	0.6530	1.3210	0.6510	1.4300	1.5605
	6	0.2700	0.7600	1.5690	0.6500	0.7390	0.6510	1.9200	2.1755
Temple	8	0.3000	0.8100	1.5800	0.7400	0.7600	0.6890	3.0805	3.5605
	10	0.4400	1.3800	2.3500	1.0690	0.7600	0.8100	3.7715	4.9285
	12	0.3600	0.8600	1.7200	0.7710	0.8000	0.7300	3.5765	4.2245
	4	0.4250	1.1510	2.8120	0.8400	0.8710	0.8550	2.1855	2.2690
	6	0.2700	0.7900	1.6000	0.7200	0.7700	0.7400	2.0005	3.2575
Flower	8	0.3860	0.9860	2.5490	1.5090	0.8630	0.7330	4.1070	4.4885
	10	0.8540	1.6520	2.4080	0.9010	1.3190	1.5640	4.8340	4.6935
	12	0.5600	1.1700	2.1900	1.1300	0.8700	1.0000	3.7055	4.0505
	4	0.4700	1.1750	2.8030	0.7110	0.9170	0.8500	2.2840	2.2155
	6	0.5170	0.9080	2.4520	0.7370	0.8370	0.7510	2.5625	2.1245
Mountain	8	0.2920	0.8200	1.7150	0.6800	0.9710	0.8810	3.3625	2.8755
	10	0.4300	0.8200	3.4100	0.7100	0.8010	0.8800	5.0305	4.2160
	12	0.4000	0.8820	1.5710	0.7900	1.1500	0.8550	4.4010	3.9205
	4	0.4500	0.9200	1.9700	0.9800	1.5640	0.7900	1.6595	2.3955
	6	0.4300	1.0950	2.6590	1.7460	1.0490	1.6700	3.1700	3.5230
Tree	8	0.3410	1.4480	2.8000	0.9750	0.7530	0.6930	2.6675	3.7390
	10	0.3740	1.2760	2.3920	0.8310	0.8920	0.8130	3.6270	3.5155
	12	0.4500	0.9390	0.9390	0.9390	0.8990	0.8510	3.9570	5.2985
	4	0.4040	0.8970	1.8600	0.6840	0.7480	0.9190	1.7475	1.8105
	6	0.3140	0.8380	1.6460	0.8150	0.7450	0.6850	2.0365	2.2195
Horse	8	0.3010	1.0490	1.8420	0.7300	0.8770	0.7740	3.2820	2.9730
	10	0.3300	0.8560	1.6410	0.7780	0.8540	0.7920	3.7315	3.8360
	12	0.3920	0.9120	1.7110	1.6600	1.6600	1.0670	4.2670	4.8615

Continued on next page

Image	K	SSA	MVO	DA	FPA	PSO	SCA	ALO	MALO
	4	0.4200	1.9550	2.5860	1.7110	0.9140	0.7110	1.6845	1.8555
	6	0.2660	0.8010	1.5530	0.7070	1.3360	1.0980	2.8115	3.0780
Bridge	8	0.3210	0.9610	2.7830	1.0120	0.9970	0.7930	4.5400	4.8560
	10	0.4110	1.5550	2.6160	1.0420	1.6320	0.9770	5.2685	5.8515
	12	0.5330	1.2210	2.9890	1.1920	1.9340	1.1170	4.6090	4.1150
	4	0.4400	0.9200	2.3630	0.7820	1.0780	0.8350	1.8890	1.8405
	6	0.2810	1.6590	2.2270	0.7510	1.3550	0.8610	3.4105	2.8835
Pilot	8	0.4400	1.5610	2.2130	0.8350	1.0880	1.2600	3.6285	3.9075
	10	0.3700	1.0850	2.7580	1.2330	1.2590	1.3200	4.9585	5.6945
	12	0.3740	0.9200	1.7840	1.2990	1.1100	1.5060	5.2780	4.0805
	4	0.4500	1.0160	2.4440	0.8390	0.8300	1.3690	1.7170	2.5915
	6	0.2750	1.3830	2.4210	1.2500	0.8100	1.3300	3.1915	3.4480
Dog	8	0.4700	0.9450	1.5800	0.7400	0.7400	0.7510	2.4325	2.8155
	10	0.3490	0.8300	1.5390	0.7190	0.8010	0.7220	3.0855	3.5100
	12	0.3300	0.8720	1.5700	0.7600	0.8700	0.7800	3.7950	4.3600

Table 6. The average computational time (in second) of each algorithm using Kapur's entropy.

Image	K	SSA	MVO	DA	FPA	PSO	SCA	ALO	MALO
	4	0.6400	1.2900	1.9500	0.8000	1.6930	0.7800	1.5150	1.8455
	6	0.4700	0.8500	1.5890	0.8210	0.8910	0.7900	2.0750	2.3905
Cactus	8	0.4900	0.9500	1.6810	0.8110	0.8900	0.8080	2.4650	4.2290
	10	0.6230	1.2750	2.0900	1.0400	0.9900	0.8490	3.1220	3.6495
	12	0.5380	1.0030	1.7180	0.9570	1.0110	0.8900	3.6600	4.1195
	4	0.5800	0.9600	1.8620	0.8300	0.8900	1.4690	2.2225	2.3925
	6	0.9260	1.2200	2.6770	1.4180	0.9600	1.0310	3.2235	2.9170
Kangaroo	8	0.4800	0.8900	1.6200	0.8200	0.9000	1.1690	2.5200	3.1900
	10	0.5210	0.9200	1.6400	0.8900	0.8700	0.8400	3.0550	3.6250
	12	0.5200	0.9900	1.7500	0.8800	0.9400	0.8900	3.6400	4.1070
	4	0.6100	1.6350	2.5860	1.2700	1.2480	0.9400	2.4355	2.8155
	6	0.4700	1.0400	2.3770	1.0500	1.2900	0.7900	2.0400	2.4100
Temple	8	0.4700	0.9100	1.6800	0.8000	0.8900	0.8000	2.4900	2.9895
	10	0.5200	0.9300	1.6500	0.8600	1.0000	0.8400	3.1050	3.6095
	12	0.5700	1.0000	1.8200	0.9300	0.9100	0.8700	5.4985	4.5950
	4	0.6000	1.4130	2.6960	1.0000	1.2850	1.3000	2.3625	2.8995
	6	1.0690	0.9900	2.8420	0.9500	0.9390	0.9860	2.6195	2.7010
Flower	8	0.4800	0.9900	1.7200	0.9400	0.9200	0.8700	2.6020	3.0850
	10	0.5300	0.9700	1.8010	0.9100	0.9990	0.9600	3.2255	3.6850
	12	0.6100	1.0700	1.8100	0.9400	1.0000	1.3790	5.1945	4.5065

Continued on next page

Image	K	SSA	MVO	DA	FPA	PSO	SCA	ALO	MALO
	4	0.5600	1.5490	1.9920	0.8570	0.8810	0.8310	1.5315	1.9575
	6	0.4410	0.9230	1.7220	0.9020	0.8820	0.8800	2.0330	2.4990
Mountain	8	0.5100	0.9710	1.7300	0.9000	0.9520	0.8420	2.5850	3.1700
	10	0.5480	1.0300	1.7900	0.9040	0.9510	0.9000	5.1080	4.0555
	12	1.0660	1.0420	1.9110	0.9610	1.0690	0.9580	3.9095	4.3645
	4	0.6200	1.3020	2.8450	1.0270	1.2090	1.3510	2.2510	2.7790
	6	0.5000	1.2040	2.6420	1.3380	1.1410	0.8990	2.1775	3.1785
Tree	8	0.5110	0.8790	1.6500	0.8300	0.8800	0.8600	2.4650	2.9350
	10	0.5000	0.9300	1.6800	0.9190	0.8500	0.9000	3.0445	3.5950
	12	0.6700	1.0090	1.8600	0.9100	0.9400	0.9400	3.7930	4.1300
	4	0.6100	1.5700	3.2080	1.5370	1.6130	0.8400	2.5665	2.8115
	6	1.0800	1.2290	2.5900	0.8000	0.8100	0.9800	2.0500	2.4145
Horse	8	0.4600	0.8900	1.6000	0.8300	0.8600	0.8900	2.6550	3.2905
	10	0.5000	0.9900	1.6400	1.1500	0.8900	0.8500	3.0550	3.6400
	12	0.5400	1.9330	2.0100	0.9800	1.0100	1.0000	3.7850	4.4105
	4	0.6000	0.9500	1.7600	0.7600	0.8100	0.7300	1.4750	1.7950
	6	0.4100	0.8400	1.5700	0.8200	0.8400	0.8000	1.9300	2.3950
Bridge	8	0.4400	0.8600	1.5900	0.8700	0.8600	0.7900	2.4900	2.9775
	10	0.4700	0.9100	1.6400	0.7900	0.9100	1.2500	3.7975	3.9840
	12	0.5230	1.0150	2.1800	0.8710	0.9340	0.9500	3.7080	4.3340
	4	0.5400	0.9400	1.7300	0.7500	1.0100	0.7700	1.4750	1.7600
	6	0.3900	0.8100	1.5500	0.8300	0.8700	0.8800	2.0940	2.5195
Pilot	8	0.4600	0.8400	1.8120	0.7760	0.9500	0.8600	2.6975	3.1400
	10	0.5650	1.1600	2.2950	0.9460	0.9790	0.9690	3.5840	4.1245
	12	0.5800	1.3060	2.3550	1.2900	1.0490	1.3350	5.6445	8.5025
	4	0.6600	1.2350	3.0700	1.0100	1.0550	1.6800	2.5700	3.0600
	6	0.5050	1.0870	2.1600	0.9200	0.9200	0.8500	2.2025	2.8425
Dog	8	0.5050	1.2550	2.9380	1.0800	1.8400	1.4900	4.5565	5.3650
	10	0.5920	1.4200	2.2400	0.9200	1.2000	0.9250	3.4000	3.9405
	12	0.5790	1.0750	1.8410	0.9500	0.9990	0.9140	3.8400	4.5330

Tables 5 and 6 show the average computational time (in second) of each algorithm using Otsu and Kapur's entropy, respectively. MALO enhanced the native ALO in many aspects, such as fitness value, PSNR, SSIM, and FSIM. However, it can be found from Tables 5 and 6 that MALO has the relatively high time consumption compared to the other algorithms. In fact, the high consumption is mainly caused by the high computational cost of the native ALO. The proposed improvement results in increasing the computational time of MALO as well. In short, in order to improve the overall performance of algorithm, it cannot guarantee to obtain optimal parameters in all cases.

Table A8 denotes the PSNR, SSIM and FSIM values obtained by MALO using the Otsu and Kapur's entropy. By comparison, it can be found that the average value of the evaluation metrics obtained by using the Otsu method is higher. For selected 10 images, using the Otsu method is just recommended. Wolpert and Macerday put forward the No Free Lunch (NFL) theorem [60]. Of course, Otsu and Kapur's entropy methods have different theoretical foundations, so the types of images they process also have

different focuses.

Tables A9 and A10 give the optimal thresholds of MALO under Otsu and Kapur's entropy at 4, 6, 8, 10, and 12 levels. Taking the "Tree" image an examples, the segmented results based on different algorithms using Otsu at 4, 6, 8, 10, and 12 levels are presented in Figure 6. Taking the "Horse" image an examples, the segmented results based on different algorithms using Kapur's entropy at 4, 6, 8, 10, and 12 levels are presented in Figure 7. Different target regions correspond to different threshold ranges. Considering the segmented images presented in Figures 6 and 7, it can be found that the images with high levels contain more information and details than that with low levels. Furthermore, the MALO based method has achieved the desired goal, because the main target areas have been efficiently identified. To sum up, the proposed method is competent for most cases and can still be considered as a competitive technique for the multilevel thresholding color image segmentation.

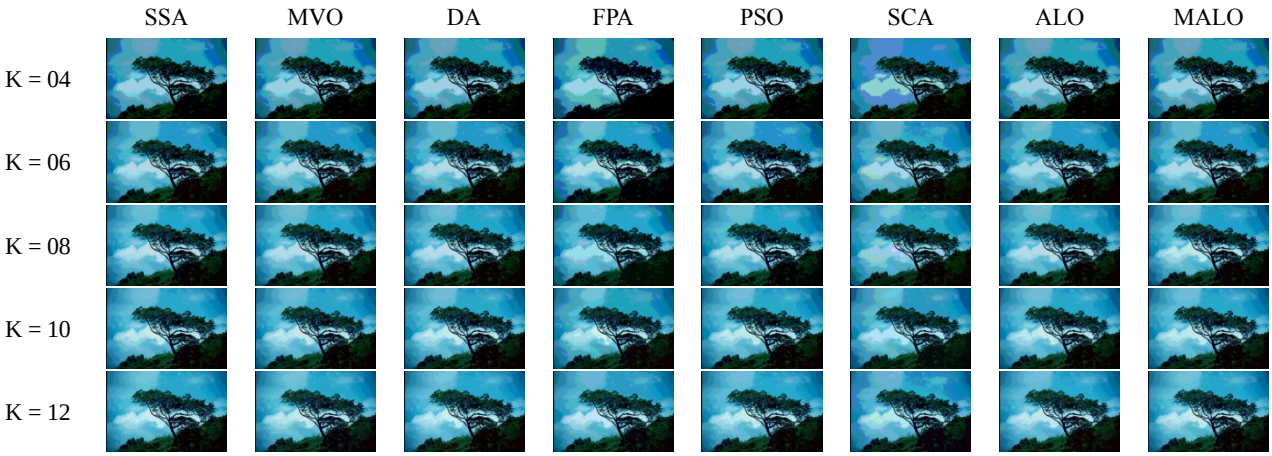

Figure 6. Segmented results of "Tree" image obtained by different algorithms using Otsu at 4, 6, 8, 10, and 12 levels.

Figure 7. Segmented results of "Horse" image obtained by different algorithms using Kapur's entropy at 4, 6, 8, 10, and 12 levels.

5.5. Comparison with improved algorithms on Berkeley images

In this subsection, the proposed method is further compared with some improved algorithms, including MABC, IDSA, WOA_TH, and BDE. PSNR and FSIM are utilized for analysis.

For visual analysis, the PSNR values obtained are represented as a line graph in Figures 8 and 9. From the figures we can observe that the MALO based method gives the higher values in general, which indicates that the segmented image is similar to the original image. For example, in the circumstance of "Flower" image through Otsu technique (for K = 12), the PSNR values are 29.5819, 29.4498, 29.3192, 29.6828, and 30.7280 for MABC, IDSA, WOA_TH, BDE, and PSO, respectively. It also can be seen that all algorithms give the similar results when the number of thresholds is small (such as K = 4). Whereas, when the number of thresholds increase, the difference between algorithms becomes greater and the MALO based method outperforms the others. On comparing the FSIM values, which are given in Figures 10 and 11, it can be observed that the values increase as the number of the thresholds increase. In the circumstance of "Temple", "Flower", "Mountain", "Tree", "Bridge", "Pilot", and "Dog" images through Otsu technique (for K = 12), the proposed algorithm is not the best. However, the proposed method gives the highest values on most cases through Kapur's entropy (for K = 12). These results indicate the precise search ability of MALO based method, which is suitable for color image segmentation.

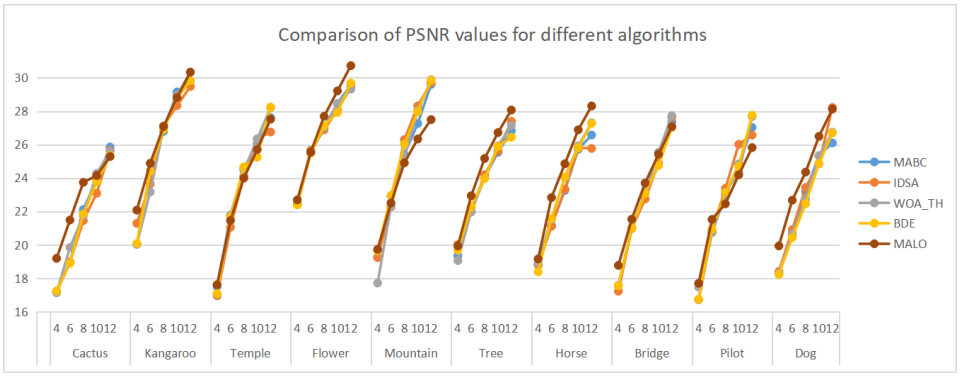

Figure 8. Comparison of PSNR values for different algorithms using Otsu at 4, 6, 8, 10, and 12 levels.

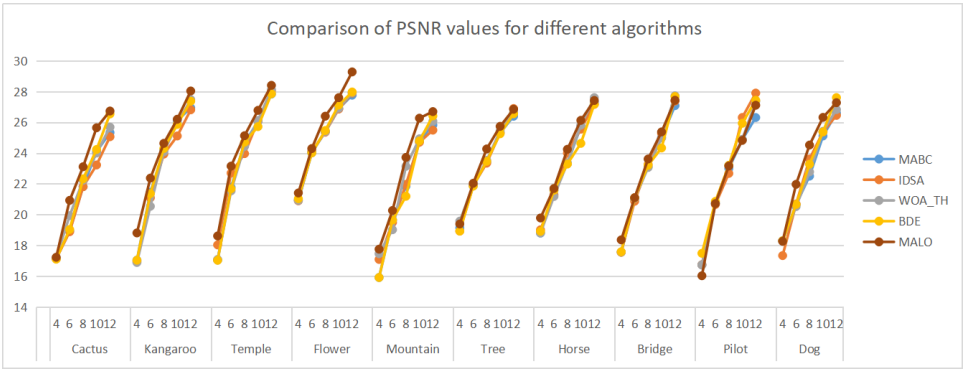

Figure 9. Comparison of PSNR values for different algorithms using Kapur's entropy at 4, 6, 8, 10, and 12 levels.

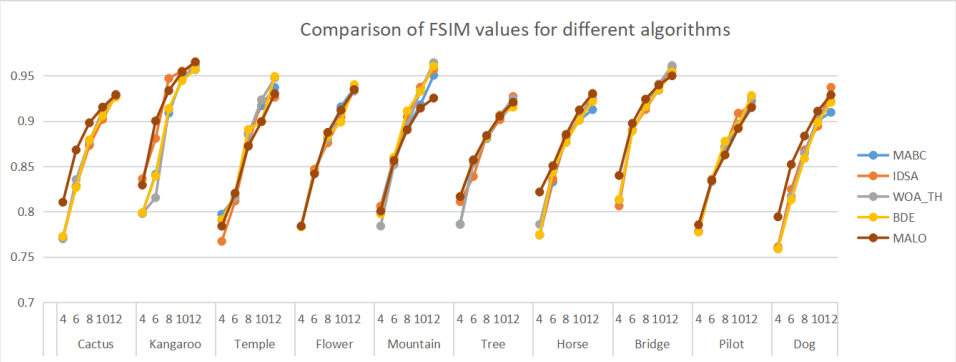

Figure 10. Comparison of FSIM values for different algorithms using Otsu at 4, 6, 8, 10, and 12 levels.

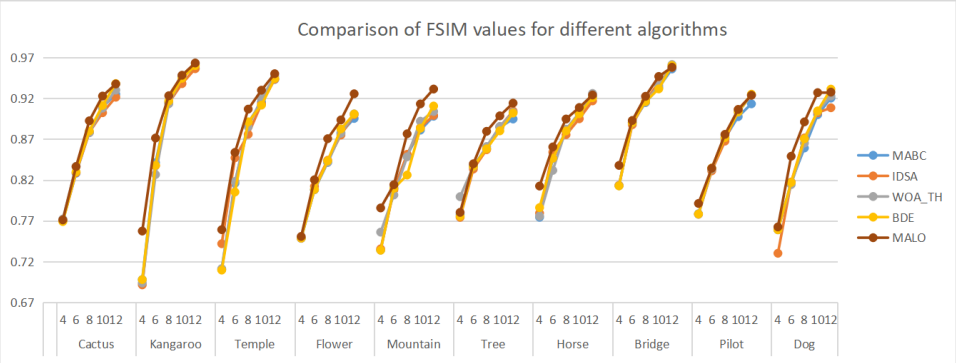

Figure 11. Comparison of FSIM values for different algorithms using Kapur's entropy at 4, 6, 8, 10, and 12 levels.

6. Conclusions

In this paper, an ant lion optimizer algorithm based on opposition-based learning for multilevel thresholding color image segmentation is proposed. Among many thresholding segmentation methods, Otsu and Kapur's entropy are adopted. The proposed algorithm is used to find the optimal threshold for 10 color test images. IEEE CEC2017 benchmark functions are performed to verify the performance of the proposed algorithm. Furthermore, 7 traditional algorithms and 4 improved algorithms are selected for comparisons. The fitness value, PSNR, SSIM, FSIM, and computational time are used to evaluate the quality of segmentation. By the convergence curve and boxplot at K=12, it can be seen that MALO algorithm can find larger objective function value more times at nearly the 100th iteration. In terms of PSNR, SSIM, and FSIM, the value obtained by the MALO algorithm is larger than other algorithms in most cases. It concludes that the segmentation performance based on MALO algorithm is superior. To sum up, a variety of experiments fully proves that MALO algorithm has higher search accuracy and convergence speed. However, high time consumption might be considered a principle limitation of this method.

In the future, the relevant research directions are given as follows:

(1) Explore to introduce other strategies and hybrid other algorithms in improving the performance of the ALO algorithm.

(2) Extend the algorithm to multi-objective problem for obtaining superior segmentation effect.

Acknowledgments

This work was supported by the Harbin Normal University doctoral research initiation fund project (XKB202014), Sanming University introduces high-level talents to start scientific research funding support project (20YG14), Guiding science and technology projects in Sanming City (2020-G-61), Educational research projects of young and middle-aged teachers in Fujian Province (JAT200618), Scientific research and development fund of Sanming University (B202009).

Conflict of interest

All authors declare no conflicts of interest in this paper.

References

1. N. M. Zaitoun, M. J. Aqel, Survey on Image Segmentation Techniques, *Procedia Comput. Sci*., **65** (2015), 797–806.
2. M. Sridevi, C. Mala, A Survey on Monochrome Image Segmentation Methods, *Procedia Technol*., **6** (2012), 548–555.
3. A. K. M. Khairuzzaman, S. Chaudhury, Multilevel thresholding using grey wolf optimizer for image segmentation, *Expert Syst. Appl*., **86** (2017), 64–76.
4. J. Tang, Y. Wang, C. Huang, H. Liu, N. Al-Nabhan, Image edge detection based on singular value feature vector and gradient operator, *Math. Biosci. Eng*., **17** (2020), 3721–3735.
5. X. Song, Y. Wang, Q. Feng, Q. Wang, *Improved graph cut model with features of superpixels and neighborhood patches for myocardium segmentation from ultrasound image*, Infinite Study, 2019.
6. X. Lu, Z. You, M. Sun, J. Wu, Z. Zhang, Breast cancer mitotic cell detection using cascade convolutional neural network with U-Net, *Math. Biosci. Eng*., **18** (2021), 673–695.
7. H. Jia, K. Sun, W. Song, X. Peng, C. Lang, Y. Li, Multi-Strategy Emperor Penguin Optimizer for RGB Histogram-Based Color Satellite Image Segmentation Using Masi Entropy, *IEEE Access*, **7** (2019), 134448–134474.
8. S. Wang, H. Jia, X. Peng, Modified salp swarm algorithm based multilevel thresholding for color image segmentation, *Math. Biosci. Eng*., **17** (2019), 700–724.
9. A. Dirami, K. Hammouche, M. Diaf, P. Siarry, Fast multilevel thresholding for image segmentation through a multiphase level set method, *Signal Process*., **93** (2013), 139–153.
10. E. Hamuda, M. Glavin, E. Jones, A survey of image processing techniques for plant extraction and segmentation in the field, *Comput. Electron. Agric*., **125** (2016), 184–199.
11. S. Kotte, R. K. Pullakura, S. K. Injeti, Optimal multilevel thresholding selection for brain MRI image segmentation based on adaptive wind driven optimization, *Measurement*, **130** (2018), 340–361.
12. N. Otsu, A threshold selection method from gray-level histograms, *IEEE Trans. Syst. Man Cybern*., **9** (1979), 62–66.
13. J. N. Kapur, P. Sahoo, A. K. C. Wong, A new method for gray-level picture thresholding using the entropy of the histogram, *Comput. Vis. Graph Image Process*., **29** (1985), 273–285.

14. A. K.Bhandari, V. K. Singh, A. Kumar, G. K. Singh, Cuckoo search algorithm and wind driven optimization based study of satellite image segmentation for multilevel thresholding using Kapur's entropy, *Expert Syst. Appl*., **41** (2014), 3538–3560.
15. M. A. E. Aziz, A. A. Ewees, A. E. Hassanien, Whale Optimization Algorithm and Moth-Flame Optimization for multilevel thresholding image segmentation, *Expert Syst. Appl*., **83** (2017), 242–256.
16. K. P. Baby Resma, M. S. Nair, Multilevel thresholding for image segmentation using Krill Herd Optimization algorithm, *J. King Saud Univ. Comput. Inf. Sci*., (2018), forthcoming.
17. A. Ibrahim, A. Ahmed, S. Hussein, A. E. Hassanien, Fish image segmentation using Salp Swarm Algorithm, in *The International Conference on Advanced Machine Learning Technologies and Applications (AMLTA2018)*, Springer, (2018), 42–51.
18. S. Ouadfel, A. Taleb-Ahmed, Social spiders optimization and flower pollination algorithm for multilevel image thresholding: A performance study, *Expert Syst. Appl*., **55** (2016), 566–584.
19. M. Díaz-Cortés, N. Ortega-Sánchez, S. Hinojosa, D. Oliva, E. Cuevas, R. Rojas, et al., A multi-level thresholding method for breast thermograms analysis using Dragonfly algorithm, *Infrared Phys. Technol*., **93** (2018), 346–361.
20. S. C. Satapathy, N. Sri Madhava Raja, V. Rajinikanth, A. S. Ashour, N. Dey, Multi-level image thresholding using Otsu and chaotic bat algorithm, *Neural Comput. Appl*., **29** (2018), 1285–1307.
21. M. Salvi, F. Molinari, Multi-tissue and multi-scale approach for nuclei segmentation in H&E stained images, *BioMed. Eng. OnLine.*, **17** (2018), 89.
22. Y. Feng, H. Zhao, X. Li, X. Zhang, H. Li, A multi-scale 3D Otsu thresholding algorithm for medical image segmentation, *Digital Signal Process*., **60** (2017), 186–199.
23. D. Zhao, L. Liu, F. Yu, A. A. Heidari, M. Wang, G. Liang, et al., Chaotic random spare ant colony optimization for multi-threshold image segmentation of 2D Kapur entropy, *Knowl. Based Syst*., **216** (2021), 106510.
24. D. Zhao, L. Liu, F. Yu, A. A. Heidari, M. Wang, D. Oliva, et al., Ant colony optimization with horizontal and vertical crossover search: Fundamental visions for multi-threshold image segmentation, *Expert Syst. Appl*., **167** (2021), 114122.
25. L. He, S. Huang, An efficient krill herd algorithm for color image multilevel thresholding segmentation problem, *Appl. Soft Comput*., **89** (2020), 106063.
26. I. Hilali-Jaghdam, A. B. Ishak, S. Abdel-Khalek, A. Jamal, Quantum and classical genetic algorithms for multilevel segmentation of medical images: A comparative study, *Comput. Commun*., **162** (2020), 83–93.
27. B. Wu, J. Zhou, X. Ji, Y. Yin, X. Shen, An ameliorated teaching-learning-based optimization algorithm based study of image segmentation for multilevel thresholding using Kapur's entropy and Otsu's between class variance, *Inf. Sci*., **533** (2020), 72–107.
28. S. Mirjalili, The Ant Lion Optimizer, *Adv. Eng. Software*, **83** (2015), 80–98.
29. M. J. Hadidian-Moghaddam, S. Arabi-Nowdeh, M. Bigdeli, D. Azizian, A multi-objective optimal sizing and siting of distributed generation using ant lion optimization technique, *Ain Shams Eng. J.*, **9** (2018), 2101–2109.
30. M. Raju, L. C. Saikia, N. Sinha, Automatic generation control of a multi-area system using ant lion optimizer algorithm based PID plus second order derivative controller, *Int. J. Electr. Power Energy Syst*., **80** (2016), 52–63.

31. P. Saxena, A. Kothari, Ant Lion Optimization algorithm to control side lobe level and null depths in linear antenna arrays, *Int. J. Electron. Commun*., **70** (2016), 1339–1349 .
32. E. Umamaheswari, S. Ganesan, M. Abirami, S. Subramanian, Cost Effective Integrated Maintenance Scheduling in Power Systems using Ant Lion Optimizer, *Energy Procedia*, **117** (2017), 501–508.
33. P. D. P. Reddy, V. C. V. Reddy, T. G. Manohar, Ant Lion optimization algorithm for optimal sizing of renewable energy resources for loss reduction in distribution systems, *J. Electr. Syst. Inf. Technol*., **5** (2018), 663–680.
34. D. Oliva, S. Hinojosa, M. A. Elaziz, N. Ortega-Sánchez, Context based image segmentation using antlion optimization and sine cosine algorithm, *Multimedia Tools Appl*., **77** (2018), 25761–25797.
35. C. Jin, Z. Ye, L. Yan, Y. Cao, A. Zhang, L. Ma, et al., Image Segmentation Using Fuzzy C-means Optimized by Ant Lion Optimization, in *2019 10th IEEE International Conference on Intelligent Data Acquisition and Advanced Computing Systems: Technology and Applications (IDAACS)*, IEEE, (2019), 388–393.
36. X. Yue, H. Zhang, A Novel Industrial Image Contrast Enhancement Technique Based on an Improved Ant Lion Optimizer, *Arab J. Sci. Eng*., 46 (2021), 3235–3246.
37. Z. Wu, D. Yu, X. Kang, Parameter identification of photovoltaic cell model based on improved ant lion optimizer, *Energy Convers. Manage*., **151** (2017), 107–115.
38. K. R. Subhashini, J. K. Satapathy, Development of an Enhanced Ant Lion Optimization Algorithm and its Application in Antenna Array Synthesis, *Appl. Soft Comput*., **59** (2017), 153–173.
39. S. K. Majhi, S. Biswal, Optimal cluster analysis using hybrid K-Means and Ant Lion Optimizer, *Karbala Int. J. Mod. Sci.*, **4** (2018), 347–360.
40. R. Sarkhel, N. Das, A. K. Saha, M. Nasipuri, An improved Harmony Search Algorithm embedded with a novel piecewise opposition based learning algorithm, *Eng. Appl. Artif. Intell*., **67** (2018), 317–330.
41. A. A. Ewees, M. A. Elaziz, E. H. Houssein, Improved grasshopper optimization algorithm using opposition-based learning, *Expert Syst. Appl*., **112** (2018), 156–172.
42. M. A. Ahandani, Opposition-based learning in the shuffled bidirectional differential evolution algorithm, *Swarm Evol. Comput*., **26** (2016), 64–85.
43. N. H. Awad, M. Z. Ali, P. N. Suganthan, Ensemble sinusoidal differential covariance matrix adaptation with Euclidean neighborhood for solving CEC2017 benchmark problems, in *2017 IEEE Congress on Evolutionary Computation (CEC)*, IEEE, (2017), 372–379.
44. R. Roy, S. Laha, Optimization of Stego image retaining secret information using genetic algorithm with 8-connected PSNR, *Procedia Comput. Sci*., **60** (2015), 468–477.
45. A. Tanchenko, Visual-PSNR measure of image quality, *J. Visual Commun. Image Represent*., **25** (2014), 874–878.
46. Z. Wang, A. C. Bovik, H. R. Sheikh, E. P. Simoncelli, Image quality assessment: from error visibility to structural similarity, *IEEE Trans. Image Process*., **13** (2004), 600–612.
47. V. Bruni, D. Vitulano, An entropy based approach for SSIM speed up, *Signal Process*., **135** (2017), 198–209.
48. C. Li, A. C. Bovik, Content-partitioned structural similarity index for image quality assessment, *Signal Process. Image Commun*., **25** (2010), 517–526.
49. L. Zhang, L. Zhang, X. Mou, D. Zhang, FSIM: A feature similarity index for image quality assessment, *IEEE Trans. Image Process*., **20** (2011), 2378–2386.

50. J. John, M. S. Nair, P. R. A. Kumar, M. Wilscy, A novel approach for detection and delineation of cell nuclei using feature similarity index measure, *Biocybern. Biomed. Eng*., **36** (2016), 76–88.
51. S. K. Dinkar, K. Deep, Opposition based Laplacian Ant Lion Optimizer, *J. Comput. Sci*., **23** (2017), 71–90.
52. M. Wang, X. Zhao, A. A. Heidari, H. Chen, Evaluation of constraint in photovoltaic models by exploiting an enhanced ant lion optimizer, *Sol. Energy*, **211** (2020), 503–521.
53. The Berkeley Segmentation Dataset and Benchmark. Available from: https://www2.eecs.berkeley.edu/Research/Projects/CS/vision/bsds/.
54. H. Jia, X. Peng, W. Song, C. Lang, Z. Xing, K. Sun, Multiverse Optimization Algorithm Based on Lévy Flight Improvement for Multithreshold Color Image Segmentation, *IEEE Access*, **7** (2019), 32805–32844.
55. A. K. M. Khairuzzaman, S. Chaudhury, Masi entropy based multilevel thresholding for image segmentation, *Multimed. Tools Appl*., **78** (2019), 33573–33591.
56. A. K. Bhandari, A. Kumar, G. K. Singh, Modified artificial bee colony based computationally efficient multilevel thresholding for satellite image segmentation using Kapur's, Otsu and Tsallis functions, *Expert Syst. Appl*., **42** (2015), 1573–1601.
57. S. Kotte, P. R. Kumar, S. K. Injeti, An efficient approach for optimal multilevel thresholding selection for gray scale images based on improved differential search algorithm, *Ain Shams Eng. J*., **9** (2018), 1043–1067.
58. V. K. Bohat, K. V. Arya, A new heuristic for multilevel thresholding of images, *Expert Syst. Appl*., **117** (2019), 176–203.
59. A. K. Bhandari, A novel beta differential evolution algorithm-based fast multilevel thresholding for color image segmentation, *Neural Comput. Appl*., **32** (2020), 4583–4613.
60. D. H. Wolpert, W. G. Macready, No free lunch theorems for optimization, *IEEE Trans. Evol. Comput*., **1** (1997), 67–82.

Appendix

Table A1. The main notations involved in this paper.

Provenance	Symbols	Paraphrase
Color images	L	The gray value
	n_i	The number of pixels with gray value of i
	N	The total number of pixels
	p	The distribution probability of gray value
	K	The total number of threshold
	t	The threshold
	C	The class
	R,G,B	The three channels of color images
Otsu	ω	The probabilities of class occurrence
	μ	The levels of class
	σ^2	The total variance
Kapur's entropy	ψ	The total entropy
ALO	X	The array of random walk
	ub	The upper bound of parameter
	lb	The lower bound of parameter
	t	The current iteration
	T	The maximum of iterations
	I	The ratio of boundary contraction
Time complexity	O	The complexity notation
PSNR	MSE	The mean square error
SSIM	R	The original image
	I	The segmented image
	μ_R, μ_I	The average gray values of image
	σ_R^2, σ_I^2	The variance of image
	σ_{RI}	The covariance of image
FSIM	PC	Phase congruency
	GM	Gradient magnitude
	Ω	The entire domain of image
	$S_L(x)$	The similarity value of each position x
	$PC_m(\mathrm{x})$	The phase consistency measure
	$S_{PC}(\mathrm{x})$	The similarity measure of phase consistency
	$S_G(\mathrm{x})$	The similarity measure of gradient magnitude

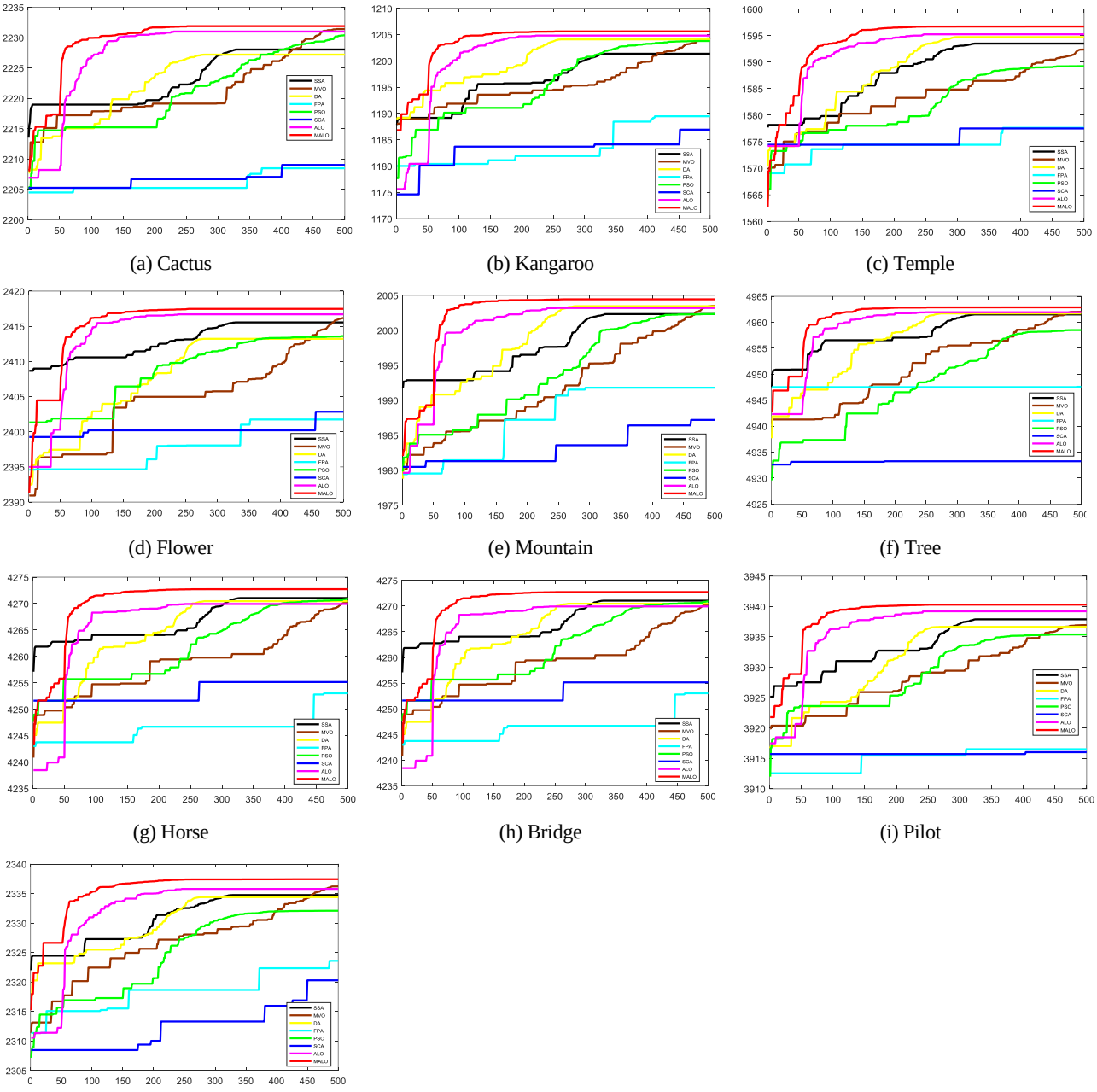

(a) Cactus (b) Kangaroo (c) Temple

(d) Flower (e) Mountain (f) Tree

(g) Horse (h) Bridge (i) Pilot

(j) Dog

Figure A1. Convergence curves for fitness values using Otsu at 12 levels thresholding.

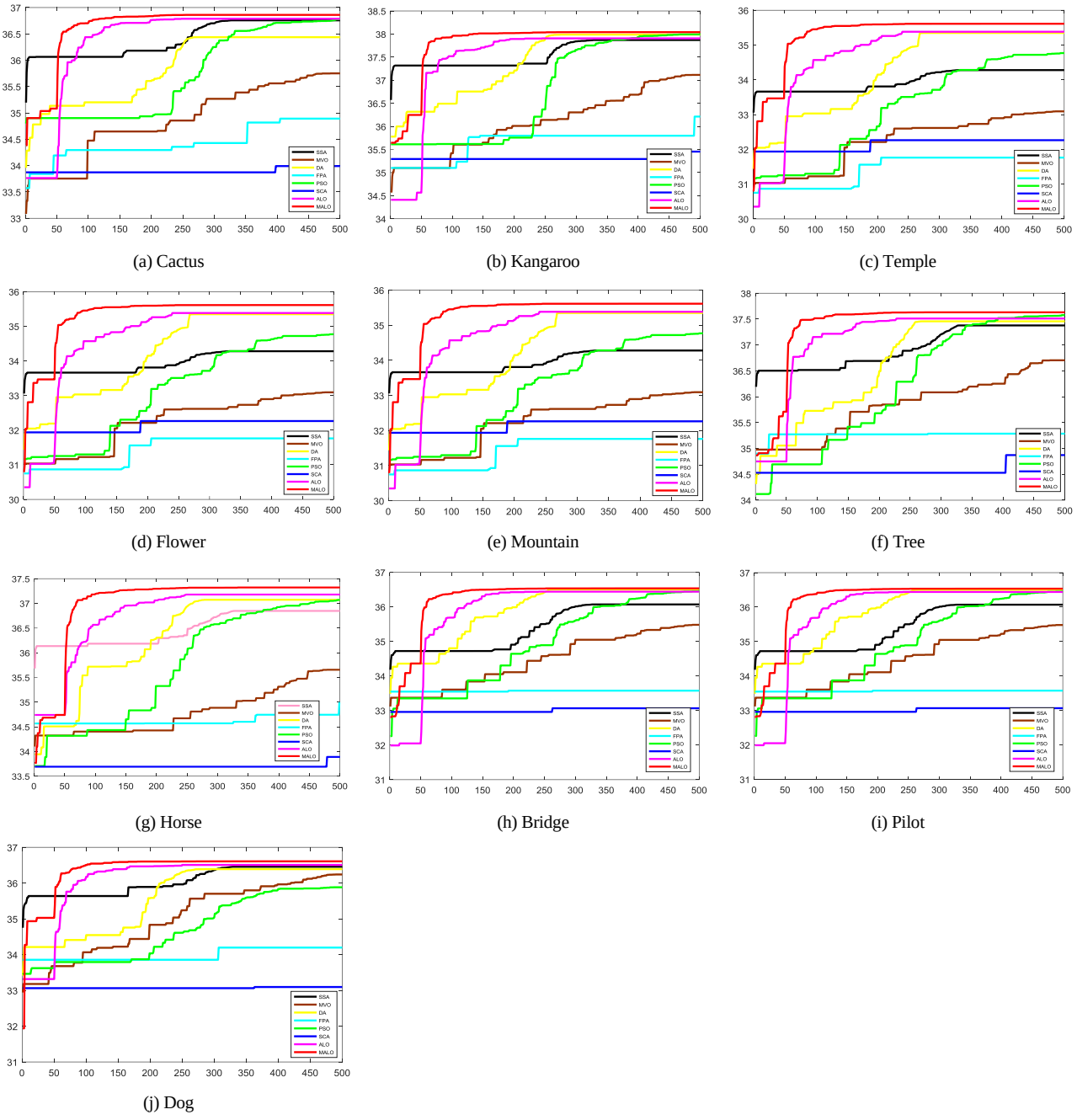

(a) Cactus (b) Kangaroo (c) Temple

(d) Flower (e) Mountain (f) Tree

(g) Horse (h) Bridge (i) Pilot

(j) Dog

Figure A2. Convergence curves for fitness values using Kapur's entropy at 12 levels thresholding.

Table A2. Comparison of PSNR values obtained with each algorithm for Otsu.

IMAGE	K	SSA	MVO	DA	FPA	PSO	SCA	ALO	MALO
	4	19.1730	19.1730	19.1730	18.7263	19.1730	18.8974	19.1344	**19.1901**
	6	21.4834	21.4806	21.4819	20.6216	21.0808	20.2685	21.4733	**21.4849**
Cactus	8	22.9129	23.0452	22.5947	21.8482	22.5738	23.0573	22.9754	**23.7403**
	10	23.8232	24.1443	23.9252	23.1394	23.9100	23.8865	24.0865	**24.1499**
	12	24.6895	25.1475	24.8778	24.9636	24.5394	25.1646	25.0007	**25.2868**
	4	22.0643	22.0643	22.0643	20.7955	22.0643	20.4905	22.0429	**22.0797**
	6	24.8251	24.8350	24.5043	23.2999	24.4744	23.1015	24.8199	**24.8836**
Kangaroo	8	26.8199	27.0457	26.8403	24.3867	26.3434	24.2914	26.9047	**27.0860**
	10	28.1619	28.8131	28.5707	25.1187	28.1677	25.2235	28.4114	**28.8186**
	12	29.1767	30.0207	29.8385	27.1879	29.8151	26.9052	30.1672	**30.3411**
	4	17.4713	17.4707	17.4713	**19.7885**	17.4736	17.1516	17.4005	17.6125
	6	20.7143	19.8002	20.7137	20.7876	19.7566	18.2250	20.7661	**21.4589**
Temple	8	22.0492	23.5836	22.5695	20.7664	22.5250	23.8550	23.4862	**23.9977**
	10	23.2619	25.2421	24.2747	23.4468	23.3367	22.7675	24.8846	**25.7059**
	12	26.8631	26.8151	25.5113	24.5639	24.7817	26.2330	26.4459	**27.5232**
	4	22.6832	22.6832	22.6832	21.9099	22.6832	22.2661	22.6832	**22.6916**
	6	25.1802	25.5484	25.5446	23.9499	25.2590	24.5962	25.5240	**25.5506**
Flower	8	27.5586	27.3846	27.6921	25.3172	27.3576	26.1643	27.5337	**27.6960**
	10	28.6654	28.8544	29.0249	26.6791	28.8757	26.7323	29.1768	**29.2169**
	12	29.9882	30.1775	29.8010	28.1115	29.6455	27.8780	30.6120	**30.7280**
	4	**19.7307**	**19.7307**	**19.7307**	19.1368	**19.7307**	19.2754	19.7277	**19.7307**
	6	21.8240	22.4882	22.3866	20.9344	22.1794	21.8654	22.3347	**22.5039**
Mountain	8	24.8724	24.1574	24.2907	22.8823	24.0400	23.4094	24.7870	**24.9053**
	10	25.9744	26.1368	26.1295	24.6068	25.8506	23.8109	26.0493	**26.3373**
	12	27.3911	26.9209	26.9014	25.3515	26.9991	25.7124	26.8751	**27.4991**
	4	19.9284	19.9265	19.9284	19.3506	19.9206	19.0453	19.9284	**19.9364**
	6	22.9219	22.9184	22.9126	21.8322	22.4339	22.4819	22.9276	**22.9388**
Tree	8	25.1296	25.0004	25.0881	22.6562	24.4342	22.7555	25.1489	**25.1704**
	10	26.7206	26.6709	26.6389	24.1790	26.1891	24.3475	26.5608	**26.7213**
	12	27.5331	28.0382	27.7147	26.1871	27.2252	24.9152	27.8812	**28.0724**
	4	19.1095	19.1095	19.1543	18.4918	19.1095	17.8797	19.1095	**19.1569**
	6	22.6175	22.6343	22.6083	22.4411	22.6441	20.0880	22.5318	**22.8301**
Horse	8	24.8257	24.6203	24.7383	23.2636	23.7326	22.2812	24.5913	**24.8543**
	10	26.7272	26.7701	26.3299	23.8301	26.2501	23.7805	26.4699	**26.8845**
	12	28.0067	27.6999	28.1864	25.0419	28.0623	24.4077	27.5665	**28.3129**
	4	**18.7684**	**18.7684**	**18.7684**	18.1883	**18.7684**	18.3216	18.7562	**18.7684**
	6	21.0341	21.5192	21.5142	20.6458	21.5142	19.4138	21.0529	**21.5346**
Bridge	8	23.5582	22.9642	23.4355	21.6761	23.3575	20.6855	23.3521	**23.7010**
	10	25.0709	24.8332	25.2117	22.7421	24.8889	23.3572	25.3971	**25.4265**
	12	26.3616	26.8858	26.3203	25.5030	26.4849	25.2994	26.1879	**27.0756**

Continued on next page

IMAGE	K	SSA	MVO	DA	FPA	PSO	SCA	ALO	MALO
	4	16.9918	16.9918	16.9918	16.9571	16.9915	16.9918	17.0028	**17.6971**
	6	19.4806	19.6603	19.3935	18.8999	19.4660	19.4742	19.4398	**21.5230**
Pilot	8	22.1137	21.7970	21.8114	19.8872	20.9936	20.1921	21.9259	**22.4562**
	10	23.3937	23.4926	22.5532	23.4677	22.5761	22.8645	23.6086	**24.1912**
	12	24.6032	24.8457	25.4417	23.3403	23.4735	24.3050	25.6425	**25.8213**
	4	19.9346	19.9569	19.9346	**20.2544**	19.9346	18.6387	19.9734	19.9346
	6	22.5690	22.6725	22.3348	21.6363	21.7981	20.9528	22.5891	**22.6726**
Dog	8	24.3105	24.3265	24.3176	23.0185	22.9836	22.5716	24.3533	**24.3548**
	10	24.9193	26.0109	25.7454	24.4410	25.5648	23.1901	25.8904	**26.4961**
	12	26.7167	28.0094	26.3712	24.9053	26.4391	25.6498	27.6947	**28.1328**

Table A3. Comparison of PSNR values obtained with each algorithm for Kapur's entropy.

IMAGE	K	SSA	MVO	DA	FPA	PSO	SCA	ALO	MALO
	4	17.1463	17.1849	17.1849	16.6326	17.1605	16.5963	17.1918	**17.2250**
	6	18.7054	19.5152	18.8374	17.7723	18.9734	18.9692	18.9353	**20.9242**
Cactus	8	20.2196	21.8061	21.8129	20.2720	20.7186	20.1477	20.8937	**23.1098**
	10	21.6755	23.5236	23.5035	22.9740	23.3426	23.5817	23.6783	**25.6436**
	12	24.5328	25.7488	24.2717	25.8229	25.6387	22.2231	25.5971	**26.7329**
	4	18.7559	18.7559	18.7529	16.9273	18.7030	17.9415	18.7714	**18.8067**
	6	21.2093	21.9397	21.7227	20.3904	21.8062	20.1191	22.1098	**22.3708**
Kangaroo	8	23.8181	24.5562	23.9062	20.5802	24.5744	22.1074	24.4808	**24.6322**
	10	25.1196	26.0125	25.7934	25.0967	25.7309	22.8701	25.9331	**26.1974**
	12	26.6277	27.4952	27.4380	24.5722	27.3277	24.0530	27.2209	**28.0349**
	4	16.7418	18.6069	17.9079	17.7575	17.8108	16.4613	18.5579	**18.6105**
	6	20.3140	20.4895	20.3140	20.7483	20.5577	21.6953	20.6648	**23.1506**
Temple	8	24.9708	24.0553	23.2965	22.2220	24.5715	23.2979	25.0443	**25.1273**
	10	25.8405	25.8930	26.0409	23.4840	26.5620	21.8980	26.5010	**26.7757**
	12	27.0259	26.4958	27.5263	24.8266	27.3391	24.0635	27.5766	**28.4027**
	4	21.4262	21.4353	21.4262	21.0771	21.4030	**21.7291**	21.3824	21.4046
	6	23.9954	24.0070	24.0260	22.9845	23.9935	23.7137	24.0223	**24.2923**
Flower	8	25.0019	25.3825	25.3936	24.4758	25.6350	25.5636	25.5517	**26.3947**
	10	26.1749	27.0175	26.8094	25.4329	26.9897	26.1739	26.8538	**27.6016**
	12	26.8429	28.2241	27.8388	25.9058	27.9865	27.9984	27.8198	**29.2750**
	4	15.7308	16.1695	16.1695	15.1291	14.6360	17.2397	14.6863	**17.7501**
	6	19.1293	19.7275	19.3198	20.0548	19.8595	18.9344	19.2375	**20.2658**
Mountain	8	22.2621	22.4482	22.2780	20.3443	22.2996	20.2389	22.1739	**23.7160**
	10	20.8677	25.1887	23.4748	22.1128	24.6158	22.2042	24.5972	**26.2667**
	12	25.4993	26.3821	26.2452	24.7312	26.5979	22.1953	26.4684	**26.6949**
	4	19.3878	19.4098	19.3878	**19.4510**	19.3660	19.0814	19.3485	19.3878
	6	21.7283	21.9982	21.9410	20.7787	21.7496	20.5382	21.9919	**22.0355**
Tree	8	23.5510	23.6198	23.4812	22.0054	23.5766	22.2770	23.5404	**24.2661**
	10	24.8234	25.5643	25.4307	23.3183	25.4128	22.1914	25.4025	**25.7360**
	12	26.1558	26.7973	26.3433	23.9995	26.5906	24.8922	26.5045	**26.8461**
	4	18.9208	19.7557	19.0344	18.9208	19.6738	19.4317	19.5801	**19.7788**
	6	21.2581	21.6962	21.6519	19.7265	21.3967	19.8505	21.6610	**21.6974**
Horse	8	23.8699	23.6078	24.2314	22.0431	23.2680	21.4611	23.4581	**24.2427**
	10	25.5023	24.5116	25.5495	23.2916	25.8501	22.6324	26.0431	**26.1268**
	12	26.4346	25.3050	27.0205	24.1636	27.1689	24.0270	26.9024	**27.4180**
	4	17.7375	17.7101	17.7433	17.6562	17.7064	17.2277	17.7680	**18.3564**
	6	21.0395	21.0300	21.0468	20.0621	21.0612	19.8616	21.0352	**21.1004**
Bridge	8	22.8402	23.4100	23.4820	21.0220	23.3430	21.3364	23.4706	**23.6124**
	10	24.6074	24.9201	24.1982	23.1209	24.7082	23.6599	24.6209	**25.3739**
	12	25.4895	26.0580	26.3086	23.1938	26.7399	24.1204	26.4986	**27.4320**

Continued on next page

IMAGE	K	SSA	MVO	DA	FPA	PSO	SCA	ALO	MALO
	4	15.9241	15.8597	15.9653	15.5965	15.8932	15.9792	15.9532	**16.0238**
	6	19.9635	19.1615	20.4713	19.5345	20.6783	20.2829	19.8317	**20.7123**
Pilot	8	22.5976	22.0836	22.9972	22.6697	23.0674	22.7085	22.8982	**23.1598**
	10	24.5888	20.7618	24.7292	23.9268	24.7256	24.0374	24.5571	**24.8228**
	12	25.6096	24.6046	26.7532	24.9263	25.9880	25.6817	26.4241	**27.1095**
	4	18.3708	18.4828	17.6137	16.0679	18.2476	18.2657	**18.4844**	18.2605
	6	20.0477	20.7865	20.6360	19.9191	20.6773	18.4516	20.7274	**21.9672**
Dog	8	22.3956	22.5129	22.5608	22.6757	22.5483	22.5758	22.3802	**24.5205**
	10	23.4554	25.3079	24.3555	24.4406	25.4561	21.6361	24.8465	**26.3186**
	12	25.8139	26.8848	26.0117	23.2895	26.5957	23.0829	26.4860	**27.2748**

Table A4. Comparison of SSIM values obtained with each algorithm for Otsu.

IMAGE	K	SSA	MVO	DA	FPA	PSO	SCA	ALO	MALO
	4	0.6001	0.6001	0.6001	0.5854	0.6015	0.6001	0.5984	**0.6063**
	6	0.6955	0.6961	0.6950	0.6716	0.6801	0.6568	0.6956	**0.6963**
Cactus	8	0.7438	0.7515	0.7268	0.7278	0.7361	0.7507	0.7487	**0.7904**
	10	0.7684	0.7838	0.7732	0.7495	0.7745	0.7814	0.7807	**0.8391**
	12	0.8012	0.8123	0.8157	0.8272	0.7927	0.8022	0.8050	**0.8456**
	4	0.7735	0.7735	0.7735	0.7156	**0.7738**	0.7046	0.7725	0.7735
	6	0.8609	0.8615	0.8515	0.8179	0.8525	0.8033	0.8608	**0.8627**
Kangaroo	8	0.9018	0.9066	0.9029	0.8415	0.8958	0.8431	0.9041	**0.9084**
	10	0.9219	0.9325	0.9288	0.8581	0.9244	0.8658	0.9262	**0.9331**
	12	0.9352	0.9466	0.9426	0.9032	0.9449	0.9032	0.9474	**0.9495**
	4	0.5829	0.5829	0.5829	0.5906	0.5825	0.5492	0.5793	**0.6798**
	6	0.7234	0.6884	0.7242	0.7222	0.6836	0.6239	0.7249	**0.7263**
Temple	8	0.7702	0.8149	0.7873	0.7265	0.7843	0.8102	0.8121	**0.8152**
	10	0.8069	0.8561	0.8329	0.7886	0.8084	0.7752	0.8480	**0.8643**
	12	0.8823	0.8883	0.8606	0.8254	0.8453	0.8546	0.8753	**0.8917**
	4	0.4655	0.4655	0.4655	0.4194	0.4655	0.4655	0.4656	**0.4916**
	6	0.5704	0.6806	0.6789	0.4849	0.6696	0.6800	0.6765	**0.7406**
Flower	8	0.7883	0.7946	0.7974	0.6136	0.7867	0.7725	0.7911	**0.8000**
	10	0.8139	0.8286	0.8219	0.7771	0.8206	0.7406	0.8268	**0.8294**
	12	0.8364	0.8550	0.8310	0.8422	0.8372	0.8203	0.8644	**0.8682**
	4	0.6987	0.6987	0.6987	0.6715	0.6987	0.6987	0.6976	**0.7081**
	6	0.7471	0.7758	0.7691	0.7237	0.7698	0.7761	0.7705	**0.7932**
Mountain	8	0.8293	0.8166	0.8127	0.7688	0.8101	0.8206	0.8311	**0.8322**
	10	0.8442	0.8536	0.8476	0.8254	0.8524	0.8261	0.8520	**0.8603**
	12	0.8682	0.8650	0.8626	0.8273	0.8731	0.8511	0.8617	**0.8780**
	4	0.6406	0.6410	0.6406	0.6162	0.6419	0.6406	0.6412	**0.6915**
	6	0.7535	0.7538	0.7535	0.6682	0.7420	0.7454	0.7538	**0.7546**
Tree	8	0.7919	0.7890	0.7901	0.7176	0.7465	0.7515	0.7954	**0.7960**
	10	0.8229	0.8272	0.8263	0.7932	0.8190	0.8009	0.8258	**0.8281**
	12	0.8372	0.8505	0.8416	0.8307	0.8387	0.8142	0.8555	**0.8579**
	4	**0.7206**	**0.7206**	0.7203	0.6791	**0.7206**	0.7155	0.7201	**0.7206**
	6	0.7543	0.7624	0.7613	0.7617	0.7611	0.7700	0.7591	**0.7744**
Horse	8	0.8102	0.8062	0.8103	0.7689	0.7945	0.7622	0.8114	**0.8117**
	10	0.8501	0.8510	0.8505	0.8026	0.8454	0.8162	0.8523	**0.8534**
	12	0.8709	0.8769	0.8739	0.8233	0.8757	0.8161	0.8686	**0.8793**
	4	0.7286	0.7286	0.7286	0.7286	0.7286	0.7293	0.7280	**0.7398**
	6	0.8032	0.8180	0.8180	0.8022	0.8190	0.7728	0.8030	**0.8193**
Bridge	8	0.8626	0.8512	0.8566	0.8374	0.8604	0.8323	0.8620	**0.8691**
	10	0.8830	0.8909	0.8903	0.8447	0.8912	0.8886	0.8956	**0.8993**
	12	0.9021	0.9140	0.9031	0.8986	0.9041	0.9063	0.9087	**0.9226**

Continued on next page

IMAGE	K	SSA	MVO	DA	FPA	PSO	SCA	ALO	MALO
	4	0.7296	0.7296	0.7296	0.7222	0.7296	0.7296	0.7299	**0.7399**
	6	0.7854	0.7857	0.7839	0.7540	0.7852	0.7849	0.7855	**0.8224**
Pilot	8	0.8420	0.8385	0.8383	0.7887	0.8218	0.7875	0.8390	**0.8424**
	10	0.8720	0.8651	0.8607	0.8555	0.8570	0.8401	0.8737	**0.8788**
	12	0.8905	0.8996	0.8951	0.8581	0.8726	0.8668	0.8947	**0.9017**
	4	0.7003	0.7031	0.7003	0.7003	0.7003	0.6563	0.6999	**0.7428**
	6	0.7700	0.7755	0.7624	0.7684	0.7514	0.7104	0.7694	**0.7756**
Dog	8	0.8188	0.8190	0.8190	0.7735	0.7848	0.7632	0.8213	**0.8240**
	10	0.8314	0.8572	0.8510	0.8116	0.8470	0.7804	0.8544	**0.8655**
	12	0.8691	0.8928	0.8643	0.8246	0.8654	0.8566	0.8886	**0.8948**

Table A5. Comparison of SSIM values obtained with each algorithm for Kapur's entropy.

IMAGE	K	SSA	MVO	DA	FPA	PSO	SCA	ALO	MALO
	4	0.4811	0.4831	0.4831	0.4466	0.4818	0.4497	0.4835	**0.4858**
	6	0.5552	0.5975	0.5613	0.5064	0.5697	**0.7353**	0.5657	0.5690
Cactus	8	0.6254	0.7141	0.7143	0.6989	0.6473	0.6168	0.6574	**0.7681**
	10	0.7156	0.7719	0.7926	0.7684	0.7661	0.8080	0.7761	**0.8677**
	12	0.8238	0.8537	0.7953	0.8778	0.8524	0.7282	0.8510	**0.8873**
	4	0.6080	0.6080	0.6078	0.5032	0.6058	0.5645	0.6083	**0.6116**
	6	0.7320	0.7635	0.7531	0.6689	0.7565	0.6881	0.7690	**0.7782**
Kangaroo	8	0.8263	0.8498	0.8304	0.7028	0.8493	0.7534	0.8476	**0.8521**
	10	0.8632	0.8867	0.8798	0.8570	0.8798	0.7602	0.8843	**0.8913**
	12	0.8976	0.9150	0.9128	0.8380	0.9111	0.8155	0.9096	**0.9254**
	4	0.5367	0.6145	0.5713	0.5753	0.5657	0.5101	0.6117	**0.6149**
	6	0.6933	0.6996	0.6933	0.7056	0.6976	0.7261	0.7014	**0.7784**
Temple	8	0.8252	0.8034	0.7796	0.7400	0.8173	0.7918	0.8318	**0.8465**
	10	0.8469	0.8719	0.8522	0.7703	0.8665	0.7311	0.8648	**0.8787**
	12	0.8733	0.8941	0.8845	0.8153	0.8796	0.8086	0.8915	**0.9021**
	4	0.3948	0.3985	0.3948	0.3969	0.3976	0.3976	0.3950	**0.3994**
	6	0.4916	0.5129	0.4916	0.4830	0.4925	0.4923	0.4917	**0.5247**
Flower	8	0.5171	0.5986	0.5385	0.5047	0.5538	0.5388	0.5387	**0.6431**
	10	0.5589	0.6425	0.5845	0.5280	0.5968	0.5964	0.5885	**0.6606**
	12	0.5737	0.6445	0.6168	0.5823	0.6299	0.7444	0.6410	**0.7643**
	4	0.4651	0.5563	0.5563	0.4348	0.4186	0.5804	0.4192	**0.6240**
	6	0.6590	0.6916	0.6673	0.7108	0.6961	0.6653	0.6674	**0.7131**
Mountain	8	0.7628	0.7797	0.7716	0.6980	0.7612	0.7505	0.7695	**0.8259**
	10	0.7035	0.8433	0.7862	0.7690	0.8408	0.8062	0.8135	**0.8792**
	12	0.8537	0.8681	0.8645	0.8367	0.8718	0.7863	0.8668	**0.9085**
	4	0.5888	0.5906	0.5888	0.6081	0.5874	0.5888	0.5866	**0.6264**
	6	0.6716	0.6898	0.6728	0.6909	0.6708	0.6817	0.6770	**0.7219**
Tree	8	0.7080	0.7157	0.7126	0.6873	0.7171	0.7503	0.7129	**0.7737**
	10	0.7271	0.7594	0.7631	0.7740	0.7656	0.6862	0.7653	**0.8214**
	12	0.7646	0.7871	0.7772	0.7040	0.7822	0.7977	0.8101	**0.8792**
	4	0.6486	0.6486	0.6637	0.6911	0.6976	0.6675	0.6835	**0.7070**
	6	0.7287	0.7486	0.7478	0.6954	0.7414	0.7463	0.7487	**0.7802**
Horse	8	0.7789	0.7930	0.7922	0.7668	0.8010	0.7618	0.8035	**0.8335**
	10	0.8221	0.8388	0.8247	0.7824	0.8276	0.7849	0.8376	**0.8697**
	12	0.8410	0.8699	0.8567	0.7938	0.8691	0.8089	0.8598	**0.8979**
	4	0.6914	0.6927	0.6902	0.6790	0.6918	0.6897	0.6946	**0.7176**
	6	0.7909	0.7974	0.7957	0.7433	0.7926	0.7813	0.7979	**0.8053**
Bridge	8	0.8336	0.8532	0.8522	0.7775	0.8505	0.8427	0.8564	**0.8820**
	10	0.8688	0.8812	0.8598	0.8144	0.8717	0.8636	0.8878	**0.9160**
	12	0.8836	0.9044	0.9271	0.8634	0.9124	0.8837	0.9116	**0.9393**

Continued on next page

IMAGE	K	SSA	MVO	DA	FPA	PSO	SCA	ALO	MALO
	4	0.7676	0.7675	0.7665	0.7440	0.7644	0.7686	**0.7688**	0.7512
	6	0.8059	0.8241	0.8201	0.7920	0.8220	0.8259	0.7979	**0.8317**
Pilot	8	0.8584	0.8617	0.8621	0.8436	0.8620	0.8585	0.8619	**0.8672**
	10	0.8859	0.8857	0.8839	0.8781	0.8852	0.8787	0.8908	**0.8937**
	12	0.9031	0.9045	0.9100	0.8703	0.9036	0.8707	0.9009	**0.9124**
	4	0.6534	0.6534	0.6218	0.5749	0.6510	0.6471	0.6582	**0.6599**
	6	0.7021	0.7305	0.7252	0.7381	0.7333	0.6472	0.7290	**0.7797**
Dog	8	0.7768	0.7801	0.7867	0.8020	0.7815	0.7875	0.7823	**0.8486**
	10	0.8039	0.8538	0.8278	0.8369	0.8574	0.7654	0.8338	**0.9002**
	12	0.8576	0.8860	0.8706	0.8378	0.8754	0.8326	0.8720	**0.8889**

Table A6. Comparison of FSIM values obtained with each algorithm for Otsu.

IMAGE	K	SSA	MVO	DA	FPA	PSO	SCA	ALO	MALO
	4	**0.8104**	**0.8104**	**0.8104**	0.7856	**0.8104**	0.7991	0.8103	**0.8104**
	6	0.8679	0.8673	0.8676	0.8305	0.8585	0.8280	0.8676	**0.8681**
Cactus	8	0.8967	0.8978	0.8936	0.8625	0.8912	0.8869	0.8974	**0.8980**
	10	0.9133	**0.9153**	0.9143	0.8868	0.9137	0.9029	0.9148	**0.9153**
	12	0.9250	0.9261	0.9264	0.9001	0.9218	0.9111	0.9272	**0.9287**
	4	0.8293	0.8293	0.8293	0.8005	**0.8297**	0.7913	0.8284	0.8293
	6	0.8998	0.8999	0.8962	0.8585	0.8904	0.8642	0.9000	**0.9001**
Kangaroo	8	0.9325	0.9328	0.9325	0.8860	0.9246	0.8884	0.9330	**0.9335**
	10	0.9474	0.9521	0.9534	0.8914	0.9454	0.9055	0.9504	**0.9541**
	12	0.9607	0.9649	0.9638	0.9358	0.9594	0.9352	0.9630	**0.9653**
	4	0.7391	0.7391	0.7391	0.7435	0.7388	0.7130	0.7374	**0.7840**
	6	0.8178	0.7984	0.8181	0.8137	0.7968	0.7606	0.8189	**0.8203**
Temple	8	0.8420	0.8693	0.8497	0.8270	0.8491	0.8671	0.8709	**0.8722**
	10	0.8628	0.8929	0.8805	0.8614	0.8615	0.8481	0.8888	**0.8994**
	12	0.9185	0.9135	0.8967	0.8820	0.8854	0.8994	0.9085	**0.9301**
	4	0.7838	0.7838	0.7838	0.7604	0.7838	0.7726	0.7838	**0.7841**
	6	0.8402	0.8413	0.8406	0.8177	0.8356	0.8142	0.8404	**0.8418**
Flower	8	0.8829	0.8810	0.8864	0.8461	0.8790	0.8524	0.8828	**0.8874**
	10	0.9041	0.9100	0.9110	0.8639	0.9092	0.8791	0.9114	**0.9120**
	12	0.9246	0.9269	0.9191	0.8891	0.9195	0.8912	0.9333	**0.9347**
	4	**0.8006**	**0.8006**	**0.8006**	0.7658	**0.8006**	0.7918	0.7999	**0.8006**
	6	0.8426	0.8561	0.8550	0.8225	0.8494	0.8335	0.8552	**0.8563**
Mountain	8	0.8893	0.8892	0.8866	0.8570	0.8824	0.8672	0.8901	**0.8903**
	10	0.9074	0.9094	0.9083	0.8789	0.9042	0.8793	0.9078	**0.9142**
	12	0.9217	0.9217	0.9214	0.8919	0.9211	0.8941	0.9182	**0.9253**
	4	0.8055	0.8056	0.8055	0.7873	0.8060	0.8055	0.8058	**0.8166**
	6	0.8562	0.8566	0.8562	0.8218	0.8479	0.8448	0.8562	**0.8568**
Tree	8	0.8826	0.8825	0.8825	0.8408	0.8680	0.8423	0.8833	**0.8840**
	10	0.9038	0.9038	0.9041	0.8713	0.8981	0.8729	0.9026	**0.9055**
	12	0.9149	0.9203	0.9201	0.8984	0.9098	0.8789	0.9186	**0.9208**
	4	**0.8217**	**0.8217**	0.8216	0.7960	**0.8217**	0.8099	0.8213	**0.8217**
	6	0.8506	0.8504	0.8503	0.8472	0.8505	0.8388	0.8490	**0.8506**
Horse	8	0.8849	0.8801	0.8848	0.8555	0.8687	0.8423	0.8827	**0.8852**
	10	0.9120	0.9082	0.9053	0.8773	0.9053	0.8708	0.9063	**0.9122**
	12	0.9269	0.9240	0.9279	0.8886	0.9254	0.8801	0.9202	**0.9303**
	4	**0.8399**	**0.8399**	**0.8399**	0.8276	**0.8399**	0.8276	0.8397	**0.8399**
	6	0.8894	0.8971	0.8968	0.8706	0.8968	0.8613	0.8894	**0.8974**
Bridge	8	0.9235	0.9150	0.9223	0.8951	0.9203	0.8849	0.9202	**0.9241**
	10	0.9368	0.9350	0.9389	0.9098	0.9346	0.9192	0.9397	**0.9398**
	12	0.9478	0.9493	0.9470	0.9332	0.9469	0.9341	0.9453	**0.9499**

Continued on next page

IMAGE	K	SSA	MVO	DA	FPA	PSO	SCA	ALO	MALO
	4	0.7854	0.7854	0.7854	0.7765	0.7854	0.7736	0.7854	**0.7855**
	6	0.8294	0.8260	0.8290	0.8070	0.8292	0.8290	0.8295	**0.8345**
Pilot	8	0.8623	0.8623	0.8619	0.8278	0.8531	0.8277	0.8617	**0.8625**
	10	0.8890	0.8819	0.8829	0.8710	0.8788	0.8547	0.8898	**0.8918**
	12	0.9033	0.9122	0.9079	0.8714	0.8905	0.8787	0.9101	**0.9148**
	4	0.7911	0.7918	0.7911	0.7911	0.7911	0.7584	0.7911	**0.7943**
	6	0.8497	0.8519	0.8467	0.8274	0.8347	0.8092	0.8494	**0.8521**
Dog	8	0.8822	0.8793	0.8823	0.8436	0.8571	0.8452	**0.8827**	**0.8834**
	10	0.8932	0.9052	0.9049	0.8720	0.9002	0.8584	0.9050	**0.9109**
	12	0.9147	0.9277	0.9127	0.8882	0.9109	0.8965	0.9235	**0.9288**

Table A7. Comparison of FSIM values obtained with each algorithm for Kapur's entropy.

IMAGE	K	SSA	MVO	DA	FPA	PSO	SCA	ALO	MALO
	4	0.7694	0.7700	0.7700	0.7508	0.7701	0.7453	0.7708	**0.7711**
	6	0.8213	0.8263	0.8232	0.7858	0.8269	0.8315	0.8248	**0.8363**
Cactus	8	0.8598	0.8767	0.8766	0.8257	0.8672	0.8361	0.8674	**0.8924**
	10	0.8791	0.9048	0.8995	0.8791	0.9021	0.8787	0.9049	**0.9227**
	12	0.9164	0.9290	0.9154	0.9140	0.9278	0.8735	0.9260	**0.9375**
	4	0.7539	0.7539	0.7536	0.6738	0.7522	0.7172	0.7549	**0.7574**
	6	0.8466	0.8609	0.8550	0.7787	0.8574	0.8118	0.8674	**0.8713**
Kangaroo	8	0.9112	0.9218	0.9113	0.8341	0.9214	0.8522	0.9196	**0.9231**
	10	0.9366	0.9456	0.9430	0.9110	0.9427	0.8605	0.9468	**0.9482**
	12	0.9543	0.9617	0.9609	0.9105	0.9617	0.8950	0.9596	**0.9632**
	4	0.7190	0.7590	0.7310	0.7199	0.7282	0.6860	0.7570	**0.7591**
	6	0.8107	0.8139	0.8107	0.7906	0.8129	0.7971	0.8111	**0.8537**
Temple	8	0.8954	0.8796	0.8681	0.8172	0.8891	0.8519	0.8990	**0.9067**
	10	0.9103	0.9290	0.9146	0.8471	0.9256	0.7991	0.9226	**0.9299**
	12	0.9293	0.9389	0.9386	0.8743	0.9315	0.8680	0.9425	**0.9501**
	4	0.7495	0.7505	0.7495	0.7293	0.7507	0.7504	0.7505	**0.7508**
	6	0.8086	0.8097	0.8101	0.7886	0.8096	0.8024	0.8095	**0.8202**
Flower	8	0.8317	0.8419	0.8411	0.8211	0.8494	0.8519	0.8464	**0.8705**
	10	0.8605	0.8796	0.8741	0.8586	0.8784	0.8538	0.8769	**0.8935**
	12	0.8736	0.9073	0.8994	0.8478	0.9015	0.8888	0.8969	**0.9255**
	4	0.7490	0.7600	0.7600	0.7470	0.7390	0.7640	0.7385	**0.7857**
	6	0.8040	0.8101	0.8111	0.7933	0.8088	0.7753	0.8046	**0.8142**
Mountain	8	0.8467	0.8612	0.8539	0.8003	0.8485	0.8084	0.8498	**0.8765**
	10	0.8444	0.8899	0.8723	0.8368	0.8834	0.8370	0.8810	**0.9131**
	12	0.8988	0.9099	0.9081	0.8771	0.9113	0.8453	0.9067	**0.9313**
	4	0.7803	0.7816	0.7803	0.7881	0.7804	**0.7947**	0.7800	0.7803
	6	0.8303	0.8366	0.8311	0.8372	0.8304	0.8367	0.8340	**0.8398**
Tree	8	0.8575	0.8602	0.8583	0.8362	0.8606	0.8490	0.8586	**0.8795**
	10	0.8741	0.8850	0.8855	0.8588	0.8862	0.8377	0.8889	**0.8985**
	12	0.8962	0.8987	0.8983	0.8545	0.9015	0.8627	0.9035	**0.9141**
	4	0.7725	0.7725	0.7844	0.7942	0.8057	0.7902	0.7952	**0.8125**
	6	0.8344	0.8467	0.8465	0.8092	0.8422	0.8260	0.8479	**0.8604**
Horse	8	0.8722	0.8784	0.8781	0.8486	0.8800	0.8444	0.8832	**0.8946**
	10	0.8977	0.9053	0.9011	0.8600	0.9005	0.8459	0.9058	**0.9087**
	12	0.9126	0.9234	0.9201	0.8674	0.9186	0.8707	0.9207	**0.9240**
	4	0.8220	0.8221	0.8219	0.8042	0.8221	0.8083	0.8234	**0.8378**
	6	0.8894	0.8909	0.8908	0.8475	0.8897	0.8495	0.8917	**0.8928**
Bridge	8	0.9137	0.9215	0.9209	0.8719	0.9208	0.8902	0.9215	**0.9224**
	10	0.9317	0.9350	0.9277	0.8925	0.9313	0.9038	0.9353	**0.9467**
	12	0.9394	0.9567	0.9453	0.9113	0.9503	0.9190	0.9476	**0.9580**

Continued on next page

IMAGE	K	SSA	MVO	DA	FPA	PSO	SCA	ALO	MALO
	4	0.7901	0.7894	0.7893	0.7740	0.7887	0.7850	0.7874	**0.7912**
	6	0.8303	**0.8409**	0.8326	0.8103	0.8337	0.8292	0.8284	0.8343
Pilot	8	0.8726	0.8726	0.8749	0.8554	0.8755	0.8649	0.8751	**0.8758**
	10	0.8991	0.8872	0.8983	0.8829	0.8984	0.8782	0.9023	**0.9063**
	12	0.9158	0.9158	0.9225	0.8776	0.9177	0.8890	0.9175	**0.9237**
	4	0.7595	0.7594	0.7375	0.7074	0.7580	0.7413	0.7621	**0.7625**
	6	0.8043	0.8208	0.8182	0.8037	0.8205	0.7507	0.8212	**0.8490**
Dog	8	0.8582	0.8617	0.8609	0.8404	0.8615	0.8355	0.8609	**0.8911**
	10	0.8772	0.9033	0.8918	0.8788	0.9032	0.8278	0.8976	**0.9269**
	12	0.9092	0.9254	0.9151	0.8727	0.9178	0.8642	0.9187	**0.9275**

Table A8. Comparison of PSNR, SSIM, and FSIM values obtained with MALO for both Otsu and Kapur's entropy.

IMAGE	K	PSNR		SSIM		FSIM	
		Otsu	Kapur	Otsu	Kapur	Otsu	Kapur
Cactus	4	**19.1901**	17.2250	**0.6063**	0.4858	**0.8104**	0.7711
	6	**21.4849**	20.9242	**0.6963**	0.5690	**0.8681**	0.8363
	8	**23.7403**	23.1098	**0.7904**	0.7681	**0.8980**	0.8924
	10	24.1499	**25.6436**	0.8391	**0.8677**	0.9153	**0.9227**
	12	25.2868	**26.7329**	0.8456	**0.8873**	0.9287	**0.9375**
Kangaroo	4	**22.0797**	18.8067	**0.7735**	0.6116	**0.8293**	0.7574
	6	**24.8836**	22.3708	**0.8627**	0.7782	**0.9001**	0.8713
	8	**27.0860**	24.6322	**0.9084**	0.8521	**0.9335**	0.9231
	10	**28.8186**	26.1974	**0.9331**	0.8913	**0.9541**	0.9482
	12	**30.3411**	28.0349	**0.9495**	0.9254	**0.9653**	0.9632
Temple	4	17.6125	**18.6105**	**0.6798**	0.6149	**0.7840**	0.7591
	6	21.4589	**23.1506**	0.7263	**0.7784**	0.8203	**0.8537**
	8	23.9977	**25.1273**	0.8152	**0.8465**	0.8722	**0.9067**
	10	25.7059	**26.7757**	0.8643	**0.8787**	0.8994	**0.9299**
	12	27.5232	**28.4027**	0.8917	**0.9021**	0.9301	**0.9501**
Flower	4	**22.6916**	21.4046	**0.4916**	0.3994	**0.7841**	0.7508
	6	**25.5506**	24.2923	**0.7406**	0.5247	**0.8418**	0.8202
	8	**27.6960**	26.3947	**0.8000**	0.6431	**0.8874**	0.8705
	10	**29.2169**	27.6016	**0.8294**	0.6606	**0.9120**	0.8935
	12	**30.7280**	29.2750	**0.8682**	0.7643	**0.9347**	0.9255
Mountain	4	**19.7307**	17.7501	**0.7081**	0.6240	**0.8006**	0.7857
	6	**22.5039**	20.2658	**0.7932**	0.7131	**0.8563**	0.8142
	8	**24.9053**	23.7160	**0.8322**	0.8259	**0.8903**	0.8765
	10	**26.3373**	26.2667	0.8603	**0.8792**	**0.9142**	0.9131
	12	**27.4991**	26.6949	0.8780	**0.9085**	0.9253	**0.9313**
Tree	4	**19.9364**	19.3878	**0.6915**	0.6264	**0.8166**	0.7803
	6	**22.9388**	22.0355	**0.7546**	0.7219	**0.8568**	0.8398
	8	**25.1704**	24.2661	**0.7960**	0.7737	**0.8840**	0.8795
	10	**26.7213**	25.7360	**0.8281**	0.8214	**0.9055**	0.8985
	12	**28.0724**	26.8461	0.8579	**0.8792**	**0.9208**	0.9141
Horse	4	19.1569	**19.7788**	**0.7206**	0.7070	**0.8217**	0.8125
	6	**22.8301**	21.6974	0.7744	**0.7802**	0.8506	**0.8604**
	8	**24.8543**	24.2427	0.8117	**0.8335**	0.8852	**0.8946**
	10	**26.8845**	26.1268	0.8534	**0.8697**	**0.9122**	0.9087
	12	**28.3129**	27.4180	0.8793	**0.8979**	**0.9303**	0.9240

Continued on next page

IMAGE	K	PSNR		SSIM		FSIM	
		Otsu	Kapur	Otsu	Kapur	Otsu	Kapur
Bridge	4	**18.7684**	18.3564	**0.7398**	0.7176	**0.8399**	0.8378
	6	**21.5346**	21.1004	**0.8193**	0.8053	**0.8974**	0.8928
	8	**23.7010**	23.6124	0.8691	**0.8820**	**0.9241**	0.9224
	10	**25.4265**	25.3739	0.8993	**0.9160**	0.9398	**0.9467**
	12	27.0756	**27.4320**	0.9226	**0.9393**	0.9499	**0.9580**
Pilot	4	**17.6971**	16.0238	0.7399	**0.7512**	0.7855	**0.7912**
	6	**21.5230**	20.7123	0.8224	**0.8317**	**0.8345**	0.8343
	8	22.4562	**23.1598**	0.8424	**0.8672**	0.8625	**0.8758**
	10	24.1912	**24.8228**	0.8788	**0.8937**	0.8918	**0.9063**
	12	25.8213	**27.1095**	0.9017	**0.9124**	0.9148	**0.9237**
Dog	4	**19.9346**	18.2605	**0.7428**	0.6599	**0.7943**	0.7625
	6	**22.6726**	21.9672	0.7756	**0.7797**	**0.8521**	0.8490
	8	24.3548	**24.5205**	0.8240	**0.8486**	0.8834	**0.8911**
	10	**26.4961**	26.3186	0.8655	**0.9002**	0.9109	**0.9269**
	12	**28.1328**	27.2748	**0.8948**	0.8889	**0.9288**	0.9275

Table A9. Optimal thresholds found by MALO using Otsu.

IMAGE	K	R	G	B
Cactus	4	48,79,124,194	58,90,126,187	54,85,123,180
	6	40,63,85,115,155,209	50,74,97,121,159,212	46,67,88,115,146,192
	8	36,54,71,89,113,144,181,225	45,64,82,99,118,142,177,221	41,58,74,91,112,137,165,204
	10	34,49,63,77,91,109,133,160,190,227	43,58,73,87,101,115,133,159,192,228	38,51,64,77,92,111,131,153,178,214
	12	33,46,58,70,82,95,113,134,156,182,209,235	40,53,66,79,91,102,114,129,148,173,200,232	37,48,60,71,82,96,112,130,147,166,189,220
Kangaroo	4	54,87,116,155	49,87,112,143	43,72,103,145
	6	41,72,92,113,140,173	38,73,95,113,134,163	32,58,77,99,128,163
	8	34,62,80,95,111,131,156,186	32,62,82,97,111,125,145,175	28,51,67,82,100,122,148,180
	10	31,56,72,85,97,110,126,145,166,195	28,55,74,88,100,111,123,138,156,185	23,44,59,71,84,99,117,138,161,190
	12	24,47,63,76,87,97,108,122,139,157,177,206	24,47,65,79,91,101,110,120,131,145,162,187	19,37,51,63,73,84,96,111,128,147,167,196
Temple	4	80,116,152,207	81,111,141,178	62,87,115,145
	6	65,89,113,137,165,213	71,93,115,138,165,208	53,70,88,107,127,151
	8	57,75,94,112,130,149,172,216	64,81,98,115,132,150,172,210	47,61,74,89,104,120,138,157
	10	55,71,87,103,118,134,151,172,200,234	60,74,88,102,115,129,143,160,178,212	45,58,69,81,95,109,124,141,159,239
	12	51,65,78,92,105,117,130,142,156,174,201,233	57,70,83,96,108,120,133,147,162,179,201,229	42,53,61,69,79,90,101,111,122,135,148,162
Flower	4	51,98,143,201	31,69,111,168	19,44,75,119
	6	34,66,98,131,163,209	22,47,77,109,150,202	7,18,37,58,84,126
	8	30,55,79,103,129,155,182,220	10,25,45,68,92,120,159,207	6,14,26,42,59,78,102,140
	10	25,44,84,104,126,149,169,192,226	10,23,39,57,76,95,117,144,178,218	6,14,26,40,56,73,94,126,176,252
	12	21,36,53,70,87,104,122,141,159,177,201,232	9,20,33,48,63,79,95,112,133,158,187,221	5,10,16,25,36,48,60,73,90,109,139,194
Mountain	4	50,76,111,190	58,91,124,190	58,94,131,192
	6	40,58,76,100,135,201	48,69,94,118,144,204	53,76,97,125,149,196
	8	36,52,67,82,103,130,167,221	45,63,79,99,118,139,174,224	39,59,78,96,121,142,157,199
	10	34,48,60,71,84,102,123,148,187,230	2,44,62,78,96,112,124,144,182,229	38,57,75,88,105,125,143,156,183,224
	12	34,47,58,67,76,88,103,119,138,161,195,230	9,43,58,69,82,98,111,122,137,157,189,233	37,53,68,79,92,110,127,141,151,160,183,224

Continued on next page

IMAGE	K	R	G	B
Tree	4	30,67,103,155	51,106,161,207	54,120,185,225
	6	13,35,65,96,132,175	39,72,112,152,183,216	38,74,125,173,203,229
	8	12,31,52,72,94,116,148,185	36,63,98,133,161,184,207,231	30,52,81,119,157,186,208,231
	10	10,23,39,56,74,94,114,139,169, 197	30,50,73,100,127,150,169,187,208, 231	28,46,68,97,130,160,184,202,215, 234
	12	9,22,37,51,66,82,97,115,136,157, 181,203	28,45,63,84,107,130,150,166,179, 192,210,233	24,37,51,69,92,119,147,171,190, 205,217,235
Horse	4	59,100,145,193	54,94,142,190	33,61,86,147
	6	49,83,111,143,179,208	46,78,104,139,177,203	27,51,72,93,145,193
	8	42,70,93,114,139,169,194,215	38,65,89,110,137,169,193,212	23,44,63,80,101,148,189,200
	10	34,56,77,95,111,130,155,180,200, 218	30,51,71,88,103,119,143,172,194, 212	18,33,47,60,72,84,98,123,162,194
	12	29,48,67,83,98,112,127,147,168, 187,204,220	29,46,63,79,93,106,120,142,166, 185,200,215	17,31,44,56,67,78,89,103,128,164, 190,201
Bridge	4	73,113,158,216	69,109,151,210	35,75,116,159
	6	61,89,116,145,180,225	61,92,120,148,181,224	24,51,80,110,139,169
	8	55,77,99,120,142,168,198,233	52,74,96,118,140,165,197,233	17,36,58,81,105,127,148,172
	10	50,68,86,104,121,139,161,184, 211,239	48,67,86,104,122,140,160,183,211, 239	13,29,46,63,81,100,119,136,153, 174
	12	48,64,79,95,110,125,140,158,178, 199,224,246	44,60,76,91,106,122,137,154,172, 192,218,243	11,25,40,55,71,88,105,121,135,149, 166,182
Pilot	4	102,149,194,224	104,157,205,235	83,123,167,220
	6	90,120,155,191,217,234	88,117,150,187,217,239	78,111,149,181,212,243
	8	80,102,127,157,187,210,225,238	81,103,127,154,185,209,225,241	66,87,109,136,165,188,214,243
	10	77,96,116,135,157,180,200,216, 228,239	76,95,114,134,158,185,206,220,233 ,246	61,78,96,115,137,162,181,195,217, 244
	12	72,89,105,121,138,158,180,197, 212,223,232,242	72,86,100,117,136,159,184,203,216 ,226,237,248	61,77,94,112,132,154,172,185,196, 214,234,248
Dog	4	50,84,115,157	73,107,145,188	52,83,123,161
	6	38,66,89,112,133,168	61,84,108,136,161,193	45,67,93,125,156,178
	8	33,58,78,97,115,130,150,184	57,75,93,112,135,156,171,199	42,60,79,102,131,157,175 ,193
	10	30,52,70,86,102,118,132,151,183, 243	53,69,84,100,117,136,154,167,181, 207	36,49,64,80,99,122,145,163,177, 196
	12	24,42,57,71,84,97,109,121,132, 147,170,197	48,61,73,87,101,115,131,147,159, 169,183,209	33,44,57,70,83,100,121,141,157, 168,179,196

Table A10. Optimal thresholds found by MALO using Kapur's entropy.

IMAGE	K	R	G	B
Cactus	4	63,103,146,189	73,115,151,196	68,111,163,206
	6	58,92,121,153,185,216	62,92,123,151,184,215	60,95,129,162,190,222
	8	50,77,102,128,154,180,204,229	56,81,106,129,152,177,202,226	19,53,80,106,134,163,190,221
	10	43,63,83,103,122,143,164,185, 207,230	49,69,89,109,129,148,169,191,212, 233	19,48,71,93,115,139,163,186,208, 230
	12	17,42,64,83,101,120,139,159,178, 197,215,234	46,63,80,97,115,132,148,165,183, 201,219,237	19,42,58,76,94,112,130,148,166, 187,208,231
Kangaroo	4	52,113,158,203	51,90,138,188	40,97,150,203
	6	43,75,113,148,184,215	47,83,123,153,186,220	36,68,102,142,185,220
	8	32,58,84,113,141,169,198,227	35,61,86,113,139,168,194,220	31,57,84,108,136,165,193,220
	10	24,45,66,90,115,138,162,186,208, 231	21,42,63,86,109,133,153,175,195, 220	25,47,69,91,114,138,161,185,207, 231
	12	20,40,58,78,98,117,136,157,178, 198,215,234	17,38,56,75,94,114,132,152,171, 190,210,229	18,36,55,74,94,115,135,154,174, 194,214,233
Temple	4	74,114,153,192	82,120,158,195	46,79,113,145
	6	64,96,128,160,194,225	72,103,134,163,196,226	25,49,80,113,144,178
	8	40,65,91,116,142,166,194,225	62,89,116,143,169,196,216,236	23,44,67,89,111,133,155,178
	10	39,60,82,103,126,149,170,194, 214,235	46,68,89,109,130,151,173,196,216, 235	18,31,47,64,81,99,118,137,156,183
	12	35,51,69,88,106,125,142,159,176, 194,213,238	41,55,73,90,107,123,141,159,178,1 96,216,235	18,31,46,63,80,97,111,127,144,158, 178,187
Flower	4	53,99,143,187	49,106,153,202	27,75,118,175
	6	42,75,108,143,177,206	32,69,106,140,175,211	20,51,82,113,145,175
	8	37,65,94,121,149,177,202,227	25,54,83,112,140,169,196,223	20,47,75,102,127,150,175,197
	10	28,50,73,95,116,137,159,183,205, 228	22,45,68,92,115,138,161,184,207, 230	17,36,55,76,97,116,135,155,175, 197
	12	26,46,66,84,102,121,140,158,176, 195,214,233	20,39,58,78,98,116,136,155,175, 196,216,236	14,27,42,56,71,87,103,118,135,155, 175,198
Mountain	4	53,89,124,156	87,138,177,218	88,132,173,215
	6	53,91,129,168,199,232	73,103,138,172,207,241	19,63,95,132,173,215
	8	52,81,107,134,162,188,216,245	51,77,102,136,160,185,213,241	19,46,65,87,109,133,173,210
	10	22,51,74,97,123,147,168,192,218, 245	51,76,101,119,138,160,181,203, 223,244	19,45,65,87,109,131,151,173,199, 227
	12	21,40,60,82,103,124,145,167,185, 205,224,247	48,64,82,101,120,137,154,172,188, 206,224,244	19,45,65,89,111,132,151,172,185, 200,218,236

Continued on next page

IMAGE	K	R	G	B
Tree	4	51,92,134,182	63,112,157,206	56,99,148,192
	6	29,63,97,132,168,206	45,77,110,141,170,207	44,78,113,151,190,225
	8	25,55,83,110,134,162,190,218	39,66,94,123,152,180,206,230	38,65,91,118,145,170,196,225
	10	22,43,65,88,111,133,155,178,198,219	33,54,75,96,117,139,160,183,206,229	33,55,77,99,119,140,160,182,203,225
	12	21,42,63,84,108,131,149,167,183,200,218,235	29,47,65,83,100,117,134,152,168,187,206,230	28,46,63,81,99,119,138,156,174,190,206,225
Horse	4	52,91,136,187	68,124,176,235	53,117,174,214
	6	43,77,111,142,177,213	49,86,126,161,193,235	35,67,103,134,173,214
	8	35,62,88,115,141,169,194,222	38,67,96,127,156,184,211,235	30,59,89,114,142,173,192,214
	10	31,55,77,99,123,144,167,191,213,235	32,55,78,102,127,150,172,193,213,235	22,44,64,86,105,125,148,173,192,214
	12	27,46,66,85,104,123,142,160,178,198,219,239	28,46,64,82,100,120,136,156,176,195,215,235	19,35,51,70,87,103,119,136,155,173,190,214
Bridge	4	70,113,156,199	77,129,180,227	49,96,142,194
	6	63,98,133,167,201,236	60,93,126,159,193,230	32,62,92,122,155,194
	8	54,80,106,132,158,184,209,236	52,78,105,132,158,185,210,236	26,49,73,97,121,146,171,195
	10	48,70,92,113,134,156,177,198,218,239	47,68,90,111,133,155,177,198,219,238	24,45,68,90,112,133,155,176,194,209
	12	45,62,79,97,114,132,149,167,184,201,220,239	44,62,80,99,116,134,152,169,186,204,222,240	22,40,58,74,89,105,121,139,157,176,194,209
Pilot	4	94,134,169,204	100,146,191,220	74,106,139,173
	6	81,110,139,168,197,221	81,108,135,163,192,220	41,85,125,168,203,235
	8	72,96,119,143,168,194,216,238	74,98,121,145,168,191,210,231	34,67,92,118,144,171,203,235
	10	69,87,106,125,144,164,183,202,220,238	70,89,108,127,146,164,182,200,218,236	28,42,68,91,115,139,163,182,205,235
	12	55,70,86,103,120,136,151,168,185,203,220,238	67,82,98,113,129,145,160,175,191,206,221,238	28,42,67,88,110,130,149,168,185,205,227,245
Dog	4	43,92,146,187	74,112,149,192	62,102,149,200
	6	38,73,110,145,174,206	62,90,119,150,184,215	56,91,124,157,195,217
	8	29,55,84,113,144,167,190,214	61,87,113,138,159,184,206,233	46,72,97,124,152,175,196,217
	10	21,40,60,80,100,120,144,167,190,214	55,76,99,120,140,159,182,198,215,233	18,45,68,91,114,137,157,176,196,217
	12	20,39,57,75,92,110,127,144,160,179,198,217	49,66,82,99,117,133,149,165,182,197,215,233	18,39,56,72,89,105,122,141,159,178,196,217

AIMS Press